DEVELOPMENT OF AN OPTIMUM LIMESTONE CALCINED CLAY CEMENT (LC³)

Final Year Project UG 2017

By

Fatima Imran

Humaira Maqbool

Wasiq Akram

Supervisor

Dr. Hammad Anis Khan

NUST Institute of Civil Engineering

School of Civil and Environmental Engineering

National University of Sciences and Technology,

Islamabad Pakistan

2021

This is to clarify that the Final Year Project titled

DEVELOPMENT OF AN OPTIMUM LIMESTONE CALCINED CLAY CEMENT (LC^3)

Submitted by

00000222080	Fatima Imran
00000237809	Humaira Maqbool
00000210441	Wasiq Akram

has been accepted towards the requirements for

the undergraduate degree

in

CIVIL ENGINEERING

NUST Institute of Civil Engineering

School of Civil and Environmental Engineering

National University of Sciences and Technology,

Islamabad Pakistan

2021

ACKNOWLEDGEMENT

Dedication To

Our Supervisor Dr. Hammad Anis Khan

&

Our families

ABSTRACT

This thesis presents innovation to make a combined substitution of cement with calcined clay and limestone powder in order to prepare the Limestone Calcined Clay Cement (LC^3). The aim was to overall assess the performance of these new binders having higher levels of clinker substitution. This substitution of cement will not only reduce the carbon footprint of these blends but will also utilize the locally available abundant and cheap supplementary cementitious materials (SCMs). The optimum blended mix was developed by studying the effect of the amount of clinker replacement, the ratio of the calcined clay to limestone powder, and the mineralogical composition of the clay system based on fresh properties, microstructural analysis, physical characteristics, and mechanical properties of these blends was evaluated. Scanning electron microscopy (SEM) with Energy-dispersive X-ray (EDX) and X-Ray diffraction (XRD) spectroscopies were also employed to see the morphological and mineralogical structure of the material. The replacement of cement ranged from as low as 30% to as high as 80% with variation in calcined clay to limestone powder ratio from 1:1, 2:1, and 3:1. Loss in strength and physical performance is observed when the replacement of clinker is increased beyond 50%. The thesis also studies the variation of carbon footprint and energy consumption of each blend to determine the blend with highest reduction in carbon emissions.

TABLE OF CONTENT

LIST OF FIGURES

LIST OF TABLES

LIST OF ACRONYMS

ASTM   American Society of Testing and Materials

fc'   Compressive Strength

SCM   Supplementary Cementitious Materials

LC^3 Limestone Calcined Clay Cement

OPC   Ordinary Portland Cement

XRF   X-ray fluorescence

XRD   X-ray diffraction

TGA   Thermogravimetric Analysis

SEM   Scanning Electron Microscope

EDX   Energy Dispersive X-Ray

CHAPTER 1

INTRODUCTION

1.1   Problem Statement

One of the biggest challenges that humanity is facing in the modern day is climate change. This climate change includes the global warming caused by greenhouse gases (chiefly carbon-dioxide) emitted by man-made sources, which has resulted in the shift of weather pattern. This shift in the weather pattern has disturbed the life on the sole life bearing planet Earth hence needs to be dealt with immediately. Cement industry as per current data produces about 5% of the worldwide man-made emission of CO_2, making it the one of the two biggest emitters in the world [1].

With the increase in the population there is anticipated a surge in the demand of cement. For growing and developing economies like China, India, Pakistan, Brazil, Mexico, Russia, South Africa, and Chile there is seen a trend in the growth of industries and hence these are hot markets for future mass growth of infrastructure. This economic growth along with rising personal income, GDP, and increases spending on infrastructures will drive an increase in the cement demand. This demand increases by 1% annually and will be 4.1 billion metric tons by 2023 [2]. Hence handling this increase in cement demand can be a big challenge for those countries. Moreover, the carbon emission will also increase with this huge increase in demand of cement. Keeping in view the current increase in cement demand, these needs cannot be fulfilled with conventional Portland cements with higher clinker to cement ratio. Therefore, alternatives are required which are economical, sustainable, environment friendly and are in accordance with the global concerns.

1.2   Supplementary Cementitious Materials (SCMs)

The use of Supplementary cementitious materials as a remedy for CO_2 reduction is not new but have been studied extensively [3][4]. There is a

variety of supplementary cementitious materials available in the market with varying pozzolanic properties but are not a good option for mass production because of their different availability around the globe and the final product can be even more expensive than the conventional OPC. In addition to that there is a limit to which their addition is useful in the cement system. Other than SCMs, geopolymers are considered as another alternative [5], [6]. But their use in anticipated to be from medium to large scale. Limestone calcined clay cements LC^3 are yet another alternative developed for mass production of low carbon cements. Limestone calcined clay cement (generally known as LC^3) is an innovative technology in cement industry which fulfills the need for sustainable, economical, and low carbon producing cement system that could be used on an industrial scale.

1.3   Limestone Calcined Clay Cement (LC^3) as a substitute

This thesis deals with the introduction of LC^3 technology in Pakistan, its feasibility in the local construction industry and the optimum mix design which gives the comparable strength to that of OPC. LC^3 is not just one cement product, in fact, it is the family of cements comprising of materials with different substitutes to clinker ratio. As the name suggests it uses clay, calcined at a high temperature, as a supplementary cementitious material. The combination of limestone and calcined clay makes LC^3 a compatible product to the OPC while reducing the CO_2 emission, hence saving the natural resources. Clay and limestone are already used as SCMs but the innovation lies in combining these two abundantly available resources without reducing the strength along with other mechanical properties of cement. The clay used in development of LC^3 is low grade clay hence it is available globally and its substitution in blended cement will further reduce the CO_2 emission.

1.4   Objective

To find:

1. kaolinite percentage of different clay samples
2. optimum percentage of clinker replacement in binder

3. best ratio of clay:limestone

4. Carbon footprint and Energy consumption

5. Strength development and other physical and mechanical properties

6. Microstructural properties of LC^3.

1.5　Thesis structure

Followed by introduction, a detailed literature review has been provided in chapter 2 pertaining to the materials present in LC^3.

Chapter 3 explains the material characterization utilized in the project and in- depth experimental methodology adopted for this research study comprising of casting regime and test numbers.

The results of tests and their critical explanations have been presented in chapter 4.

The conclusions drawn from this research work and recommendations for future study are summarized in chapter 5 of this thesis.

CHAPTER 2

LITERATURE REVIEW

2.1   Cement

Cement, also known as binder, is most widely used construction material that sets, hardens, and sticks to other materials in order to bind them. It is the second most consumed resource on the planet after water.

Portland cement is a type of cement generally used around the world. It is made by heating clay and limestone together at 1,500 °C in a rotary kiln. The resulting hard substance, called 'clinker', is then ground with a small amount of gypsum into a powder to make OPC (Ordinary Portland cement). Portland cement is a basic ingredient of concrete, mortar, and most non-specialty grout. The most common use for Portland cement is to make concrete, which is a composite material made of aggregate (gravel and sand), cement, and water.

Producing clinker generates 60% of the CO_2 emission[1] hence reducing the quantity of clinker and replacing it with a supplementary cementitious material will greatly reduce the amount of CO_2 emitted hence reducing its impact on the environment.[2]

The addition supplementary cementitious materials (SCMs) in the binder system is one of the most successful and effective strategy to reduce CO_2 emissions in the global cement industry. [3]

2.2   Clay

Clays have widely been used as a pozzolanic material throughout the history. Although there are many other competing materials, such as byproducts of industries, clays still are a very good option as a supplementary cementitious material.

2.2.1 Clay as Supplementary Cementitious Material

The substitution of clinker by metakaolin rich clay i.e. shifting to lower clinker/cement ratio is considered an effective way of controlling CO_2 emission [4]. One of the fundamental reason of using calcined clay for this purpose is that it does not compromise the compressive strength of the binder, in fact substitution up to 45% has better mechanical results than standard ordinary Portland cement [5].

Calcined clays, particularly in combination with limestone

2.2.2 Calcination

Calcination of clay is important to activate the pozzolanic characteristics of clay. Calcination is the heating of clay in presence of air. It results in dehydroxylation of clay minerals, hence increasing its compressive strength. If the temperature of calcination is well controlled, it can increase the performance of clay up to the level of standard OPC.

In case of kaolin the calcination temperature $550^{\circ}C$ yields compressive strength of clay to be 113% of OPC [6]. This temperature ranges to $950^{\circ}C$. Hence for the economical calcination temperature of $550\,^{\circ}C$ is generally used.

2.2.3 Pozzolanic reaction

According to ASTM C-618 the sum of $SiO_2 + AI_2O_3 + Fe_2O_3$ should be greater than 70% (ASTM C618-91, 2019) and clays present satisfactory percentage of this sum (Changling Hea, 1995). The thermal activation of clay (at $600\ ^{\circ}C$-$900\ ^{\circ}C$) results in breakdown of structure of clay, due to dehydroxylation, hence forming a new phase of increased reactivity. This phase includes metakaolin ($AI_2O_3.2\ SiO_2$) or AS_2 in kaolinite clays. The basic pozzolanic reaction includes:

$$CH + metakaolin\ (AI_2O_3.2\ SiO_2)\ + H\ \longrightarrow C\text{-}S\text{-}H + C\text{-}A\text{-}H\ [7]$$
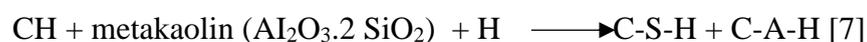
This results into formation of CSH gel along with other crystalline products including calcium aluminate hydrates and alumino-silicate hydrates. These crystalline products depend upon metakaolin to CH ratio and the temperature of reaction [8].

2.2.4 Effect of Particle Size Distribution

The fineness of clay particles play an important role in strength generation as well as heat of hydration and pore structure of the mix [9].

i.   On compressive strength:

The strength of the mix is observed to be increased for more fine clay particles as compared to the mix containing coarser particles of the calcined clay. This increase in strength is seen to be 33% at 3 day and this increment decreases with the increase of hydration period. This increases the pozzolanic properties of clay combined with the limestone, hence improving the strength overall. [9]

ii.   On heat of hydration:

Initially the heat of hydration increases as the fineness increases. This is explained by the fact that with finer particles there are more nucleation sites present for cement hydration. At 24 hours the difference is small, but this heat further increases with time. The further increment in the heat of hydration is due to the reaction of calcined clay component.[9]

iii.   On porosity:

The blend with finer particle shows high pore refinement and the porosity of the system decreases as compared to the coarser blends. This is caused by the more effective packing of the particles as small size particles fill the gap between clinker particles [10] .

2.3   Limestone

The introduction of limestone in LC^3 blend has a positive impact on the rheological properties as it reduces the flow resistance of concrete. [11]

Limestone cement concretes also indicate lower resistance to freezing and thawing compared with the pure cement concrete. Portland limestone cement, containing 20% limestone, shows the optimum protection against rebars corrosion. The limestone additions decrease the carbonation depth (carbonation depth is the average distance from the surface of concrete or mortar where carbon dioxide has reduced the alkalinity of the hydrated cement) and the total porosity of the mortar. [12]

2.4   Water Content

Water is needed to make the cement paste. The amount of water needed can greatly affect the mechanical properties of the LC^3 blend.

2.4.1 Effect of water/cement ratio:

Increase in the w/b ratio increases porosity hence decreasing the value of the compressive strength. On the other hand, a decrease in the w/c ratio increases compressive strength but also decreases workability. It was also observed in a paper that the fracture behavior of a low w/c ratio mortar is more brittle than that of a mortar with high w/c ratio. [13]

According to Abrams' generalization law, the compressive strength of concrete varies inversely with the water/cement ratio for concrete. The water–cement ratio (W/C) affects the interfacial transition zone between concrete paste and aggregate, which usually controls the strength of concrete [14]. One of the problematic issues with the use of calcined clays is the increase in the water demand due to high fineness (caused by the sheet like structure) and narrow particle size distribution.

2.5   Curing

Curing is very important for cement mortar, or concrete specimens, which influence the strength and durability development. The effect of curing temperature between 20 °C and 30 °C on the properties of LC^3 has already been studied. Increasing temperature promotes the hydration of clinker and the pozzolanic reaction resulting in a boost of strength development of LC^3 at early ages. A coarser threshold pore diameter is observed on the samples cured at 30 °C for 28 days but it does not affect the strength of LC^3. However, most of the previous tests were performed at a control temperature (20 °C) which is lower than the normal working temperature in the tropical zone countries. (Hanpongpun Wilasinee and Scrivener, 2020)

2.6   Fresh Properties of LC^3

2.6.1 Metakaolin and viscosity:

The major factor determining the fresh properties as well as strength development of LC^3 system is the metakaolin content [16]. Main reason why it is so is because MK (metakaolin) is water absorbing material and it increases the viscosity of the system [17]. The clays have the tendency to exchange cations with other added material to balance the inherent static charges present on the surface of clay. Hence when admixtures are added the clay particles readily exchange cations with the organic matter already present in the admixture introduced.

This leads to less dispersion hence less absorption of the admixture on surface hence larger dosage of admixtures are required. This higher dose can lead to increase in the cost, setting time increment and delay in strength development [18].

2.6.2 Slump:

The slump values of LC^3 system are related to the water content, super

plasticizer used but most chiefly to the metakaolin content in the mix. These slump values depend upon the morphology of the metakaolin present in the mix. When the shape of the particles is rounder and less rugged the slump increases. With increase of surface ruggedness the slump is observed to be decreased [17] .

2.6.3 Static yield strength:

Metakaolin is observed to have positive impact on the static yield strength of the fresh mix. With the increase in the amount of metakaolin the static yield strength of the mix increases. This increase in SYS is directly proportional to the resting time. The combined effect of limestone with calcined clay exhibits the best results giving highest value of SYS. Limestone has a moderate effect in increasing static yield strength over time. This is due to process of dissolution and precipitation which results in the formation of links between the grains. [19]

2.6.4 Dynamic yield stress and plastic viscosity:

The dynamic yield stress and the plastic viscosity of the mix increases with the increase in the amount of Supplementary cementitious material (clay in this case). Clays have the property to modify the viscosity and the flocculation strength. This means that as the calcined clay has direct impact on the DYS and plastic viscosity of the mix.

The role of limestone is best explained by the fact that it acts like a filler, due to its small size and hence making our mix more viscous. But the governing factor here is still the calcined clay amount [19].

2.6.5 Adhesion and Cohesion:

The combined effect of limestone and calcined clay exhibits increase in the cohesion (the ability to stick with the same substance). It is observed that the cohesion increases with the increase of SCM, whereas the addition of

limestone reduces the cohesion property of the mix.

The adhesion (ability to stick to other surfaces) of the mix increases with the increase of calcined clay [19] .

2.7   Mechanical Properties of LC^3

2.7.1 Compressive Strength:

The compressive strength of specimen is generally found by compression test in compression testing machine. Within the LC^3 system, the specimen having highest clinker amount exhibits highest compressive strength. As the amount of clinker increases the compressive strength also increases [20]

2.7.2 Flexural Strength:

The flexural strength of LC^3 specimen is more than OPC on 7 and 28 days. It shows that with addition of calcined clay the ductility of the mix increases. In the pozzolanic activity of clay the calcium hydroxide of the hydration product and calcium alumina silicate hydrates C-A-S-H are formed. This more generation of C-A-S-H products and crystalline calcium aluminates increases the flexural strength [21].

2.8   Hydration of LC^3

2.8.1 Phase assemblage:

Different phases of hydration of LC^3 can be studied by X-ray diffraction. In LC^3 system a peak of hemicarboaluminates is observed at 24 hours of hydration ($2\theta = 10.8°$)[22]. At 28 and 90 days a minor peak of monocarbonaluminates is observed ($2\theta = 11.7°$)[22], but the whole conversion of hemicarboaluminates to monocarbonaluminates is not observed. Only traces of portlandite are observed at 24 hours of hydration.

This may be due to the rapid reaction of the calcined clay present in the mix.

For characterization of C-A-S-H gel EDM/SEM (Scanning Electron Microscopy / Energy Dispersive X-Ray Spectroscopy) is used because it cannot be studied by XRD due to its amorphous nature. There is alumina present in calcined clay which modifies the structure as well as morphology of the calcium silicate hydrate, while alumina is incorporated in the gel. This alumina uptake depends upon many factors like alkali content, clay grade, the Ca/Si ratio and others. The average C-A-S-H composition at 28 days of hydration is $C_{1.61}A_{0.115}SH_X$ which shows that the alumina uptake in LC^3 is higher than that in standard OPC [22][23]

2.8.2 Alite and Belite hydration:

Quantitative rietveld analysis is used to determine the degree of hydration of alite and belite in LC^3 system. There seems to be the lower degree of hydration in later stages. When compared with OPC the hydration was found to be 15% lower. In limestone-calcined clay system the degree of hydration of belite was found to be 35% at 90 days[22]. This low hydration is more prominent when calcined clay and limestone are combined in a system. This is linked to the pore refinement that occurs due to presence of calcined clay. This pore refinement slows the hydration stages. The mercury intrusion test of the LC^3 system shows that the limiting critical pore diameter is attained in 7 days. Beyond this there is no reduction in pore size [22]

2.8.3 Reaction Kinetics:

The early hydration kinetics are studied by isothermal calorimetry. There were two peaks in the calorimetry of LC^3 system. One peak is for silicate hydration and the second peak depicts the hydration of aluminates[22]. The presence of calcined clay accelerates the hydration due to its filler nature and presence of more nucleation sites. Therefore, there is earlier generation of first hydration peak in LC^3 system as compared to OPC. A distinct second peak is observed in LC^3 system. Near onset of this peak the

depletion of sulphate occurs at 9.5 hours of addition of water [22].

2.8.4 Strength development:

Most of the compressive strength of LC^3 system is achieved within the first 28 days[24]. Calcined clay is the main reason of the production of the early strength. The strength gain between 28 and 90 days is very minimal. This is explained by the hydration of C^2S and C^3S. The pore refinement is the major limiting factor for hydration and hence strength development of the LC^3 system.

2.9 Microstructure of LC^3

Clay is a fine material. When added as a clinker substitute it greatly effects the microstructure of the matrix.

2.9.1 Porosity and Pore size distribution:

Initially the calcined clay system having different clay content shows same porosity values of 49-50%.[25] This value decreases gradually till 28 day of hydration. Beyond 28 days the porosity remains constant. The mixes having calcined clay shows total increase of porosity by 16% when compared with OPC [25].

For capillary pores (5-0.01 µm) there is no significant difference in first 7 days. After 14 days the difference between OPC and LC^3 system becomes more prominent. There is 10% increase in capillary porosity observed at this stage. But as not much difference was seen in the capillary pores of systems having 15-25% calcined clay for longer period of hydration[26].

With the incorporation of calcined clay, the pore size of the mix becomes finer. There is a prominent shift in pore size observed at 7 and 90 days which indicates the start and end of the pozzolanic activity of clay. There is a dramatic decrease in the pore size at first day of hydration. In standard OPC this reduction occurs from 1 to 56 days of hydration. For 10% metakaolin

system this pore size reduction occurs in 28 days. The pore size reduction in mixes having more than 10% stops after 14 days. The average pore size of mixes having 10% or more metakaolin is quite same[25].

2.9.2 Evolution of calcium hydroxide with time:

To determine the degree of hydration of metakaolin it is important to know the quantity of calcium hydroxide within the mix. The calcium hydroxide amount increases in the initial stages of hydration. This amount decreases with passage of time. This decrease is prominent at 56 and 90 days of hydration.

The initial increase can be justified by the hydration of OPC, which decreases as the pozzolanic activity of metakaolin increases. The inflexion points at 56 and 90 days shows the pozzolanic activity of the clay.

2.9.3 Degree of hydration:

There are different methods to find out the degree of hydration of LC^3 system.

Up to 14 days the degree of hydration is below 100% because of total absence of the pozzolanic reaction within the system[23]. Until this time the total reaction is between water and clinker particles. From 14 to 90 days this value of hydration is above 100% of standard OPC which indicates the overlap of the pozzolanic reaction and hydration of cement. Above 90 days the value of hydration becomes constant with a slight decrease for mixes having more than 20% of metakaolin.

There is a decrease in the value of degree of hydration at 90 days for mixes having low metakaolin content. This marks the end of pozzolanic reaction.

2.9.4 Relationship between porosity and degree of hydration:

Studying both the porosity and hydration with respect to time a clear

relationship can be made between them. The correlation coefficient R^2 of total, capillary, and gel pores with degree of hydration was found to be 0.71, 0.81 and 0.88 respectively[25]. Best correlation is found by gel pores then capillary pores and then total pores. This indicates that the values of degree of hydration above 100% are mainly directly related to pore refinement. This is because of increase of hydrated phases during the pozzolanic reaction [25]

2.10   Role of Gypsum

Even though gypsum is used in small percentages in cement, it plays a very important role in the different properties that are exhibited by the cement paste and its effect is predominant at the early stages. Gypsum provides workability to cement by keeping it in the plastic state during early stages of hydration therefore it is identified as a retarder or set regulator. It also contributes to the acceleration of development of strength of the paste during the early stages of hydration[27].

2.10.1 *Gypsum as a set retarder*

Without the addition of gypsum, the paste exhibits flash setting in a matter of minutes resulting from the quick hydration of calcium aluminates to form calcium aluminate hydrates. The hydration of C^3A releases heat due to it being exothermic and makes the mixture stiff which decreases the chance of remixing of the mixture. Therefore, the CAH doesn't contribute to the strength and even disables the further hydration of the calcium silicate. Therefore, this process due to the absence of gypsum makes the cement totally uneconomical and useless in the field. The following chemical equation is explanatory in this regard.

$3CaO. Al_2 O_3 + nH_2O \rightarrow$(fast reaction) CAH + profuse exothermic heat [27]
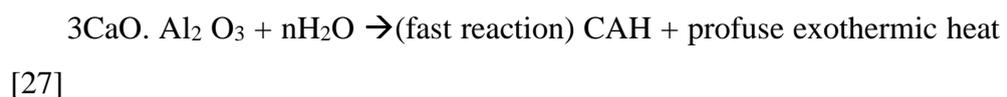
To make the cement useable, the course of reaction of C3A is to be changed which is done by the addition of sulphate salts as the C3A reacts more readily with SO3 and due to this the reaction of C3A with water is

avoided and for that purpose, gypsum is found to be the most effective form of sulphate. The chemical reaction on addition of sulphate is given below

$3CaO. Al_2O_3 + 3CaSO_4 . 2H_2O + nH_2O \rightarrow 3CaO. Al_2O_3 . 3CaSO_4 . 32H_2O$
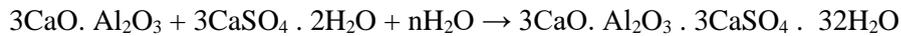
[27]

2.10.2 *Gypsum as an accelerator*

Many people just think that the role of gypsum is just as a set retarder but gypsum has another role as an accelerator for high early strength. This role generally goes unnoticed and causes the misunderstanding that the incorporation of more cement will results in further retardation of setting of the cement which is not the case. The addition of gypsum results in the formation of ettringite[27] which when produced at threshold levels accelerates the hardening process and thus quicken the early age strength gain of the paste. Hence increasing levels of gypsum is an excellent solution to overcome the weakness of paste at early ages. Therefore 5% cement is usually blended with clinker in the cement plant[27].

2.11 Superplasticizers

One of the main issue with using calcined clay is that the water demand of the paste rises due to the particles being very fine and its distribution being very narrow.[28] Therefore superplasticisers are needed in the paste to maintain the necessary workability of the paste.[29], [30] Clays have the ability to actively exchange cations to balance the electrical charge. Adding chemical admixtures replaces the cations in the clay with organic materials present in the admixture which causes a lot of the admixture being absorbed and results in higher doses of admixture is to be required causing increase in cost, delays in setting time and delays in setting times. [18] When poly-condensate and polycarboxylic ether based superplasticisers were compared on the basis of their dispersion, PCEs were observed to be more sensitive to clay.[18] It is found that PCEs undergo 100 times more physisorption and chemisorption in the presence of clay as compared to cement.[31]

The compatibility of superplasticizers with limestone metakaolin blended cement were studied by Zaribaf et al.[32] with commercially available superplasticizers namely PCE, sodium lignosulphates, naphthalene formaldehyde condensates (SNF) and polymelamine formaldehyde (SMF) with a water to binder ratio of 0.4. The dosages were tested using a mini slum test corresponding to 12cm and flow tests and were compared with control cement paste. The results showed that doses of SMF and lignosulphates required were greater than the maximum recommended doses to attain the flowability similar to control pastes. SNF and PCE based superplasticizers worked better with the blends. Increasing the level of metakaolin caused a decrease in workability and lessened the setting time which was compensated by increasing the amount of superplasticizer dosages. In that research, mortar specimens containing 30% metakaolin with PCE based superplasticizers showed an increase in compressive strength as compared to the control OPC blend.

Another study on the rheology of cement paste with metakaolin and/or limestone filler blended systems was done by Santos et al.[33] who prepared samples with metakaolin and/or limestone filler with maximum replacements up to 20% and a constant water to binder ratio of 0.3. The blends also contained 0.5 wt% of PCE superplasticizer. The research investigated fresh properties such as slump spread, march cone test, plastic viscosity, viscoelastic properties, thixotropy and yield stress. The research conducted the rheological studies using oscillatory rheometer controlled by stress. Presence of metakaolin did increase the thixotropy and plasticity of the paste but that was when the amount was 5%-8%. As beyond 10% of metakaolin adversely effected the workability of the paste and increased its yield stress. Addition of the PCE based superplasticizers improved the workability of the paste. It was concluded according to that study that a blend of 90% cement, 5% metakaolin and 5% limestone gives a good thixotropy.

A recent study looked into and compared the flowability of OPC, LC^3 and FA30 at different w/b ratios with different saturation dosages of PCE and SNF based superplasticisers.[11] The water to binder ratios were 0.35, 0.4 and 0.45. FA and LC^3 showed comparable flow times at saturation dosages and

the flow time for OPC was lesser for the saturation dosages. It was also found that the saturation dosages for SNF based super plasticizers were higher than PCE for all water to binder ratios due to the fact that PCE based superplasticisers disperse due to both steric and electrostatic repulsion forces whereas SNF based only disperse due to only electrostatic repulsion forces therefore a higher amount of SNF is required to reach the saturation point.[34], [35]

The amount of superplasticiser required for saturation was higher in LC^3 as compared to FA30 and OPC which may be due to the absorption of the superplasticiser between the layers of clay[36] and also may be explained by the increase in fineness of the LC^3 blend as the saturation point in cementitious material increase with the fineness[37]

According to this study, the mini slump values increased up to the saturation dosages. Once the saturation point was reached, there was little increase in the slump values. For very high dosages of the super plasticiser, the paste showed significant bleeding. The study concluded that LC^3 systems can reach comparable slump spreads as OPC at the saturation dosages at higher water to binder ratios[11]

This detailed literature study on the LC^3 blended cement gives an overview of the properties of the individual material used to make the blend, and their combined effect to make a sustainable blended cement. The fact that there was no study available on the effect of calcined clay to limestone ratio on the LC^3 blends makes this study more vital.

CHAPTER 3

MATERIAL AND EXPERIMENTAL METHODOLOGY

3.1 Materials

Materials used in manufacturing of LC^3 blends as well as their characterization are mentioned in the upcoming section followed by a detailed experimental methodology.

3.1.1 OPC

Since our research mixes consist of clinker and gypsum as well, hence Ordinary Portland Cement was utilized which readily had a blend of clinker and gypsum in it. Fauji cement bags were procured from a local vendor.

Xray Fluorescence (XRF) test was performed to understand the chemical composition of raw materials.

Table 3.1: Compounds in OPC

SiO2	Al2O3	Fe2O3	CaO	K2O	MnO	ZnO	SrO	MgO	Na2O
19.19	4.97	3.27	61.8	0.51	2	0.68	0.29	2.23	0.57

3.1.2 Calcined Clay

Clay from three different sites, within Islamabad, was extracted. This raw clay was not suitable to be incorporated directly in the mix because of the impurities in it and unsuitable size of the extracted lumps. Hence the impurities from the raw soil were removed, the big lumps of the soil were grinded in the ball mill and then the fine clay was sieved out of the sample through sieve # 200. After grinding and sieving the sample to required size the clay was calcined up to 850ºC in a muffle furnace. This calcination results into pozzolanic activation of the clay as the kaolinite within the clay sample dehydroxylates into metakaolin.

3.1.3 Limestone

The limestone was procured from a local vendor and was grinded and pulverized to the point that it could pass sieve # 200. That was done to make the limestone particles of the same size as those of the OPC and calcined clay.

XRF of limestone:

Table 3.2: XRF of Limestone

SiO2	Al2O3	Fe2O3	CaO	K2O	SO3	SrO	MgO	Na2O	LOI
1.08	0.14	0.13	53.24	0.04	1.59	0.29	1.49	0.03	42.256

The XRF results show maximum amounts of calcium with trace amounts of other elements.

SEM of limestone:

Scanning electron microscopy (SEM) is a technique that scans samples by using and electron beam and produces magnified images for analysis. To conduct the morphological study of our material, this test was performed.
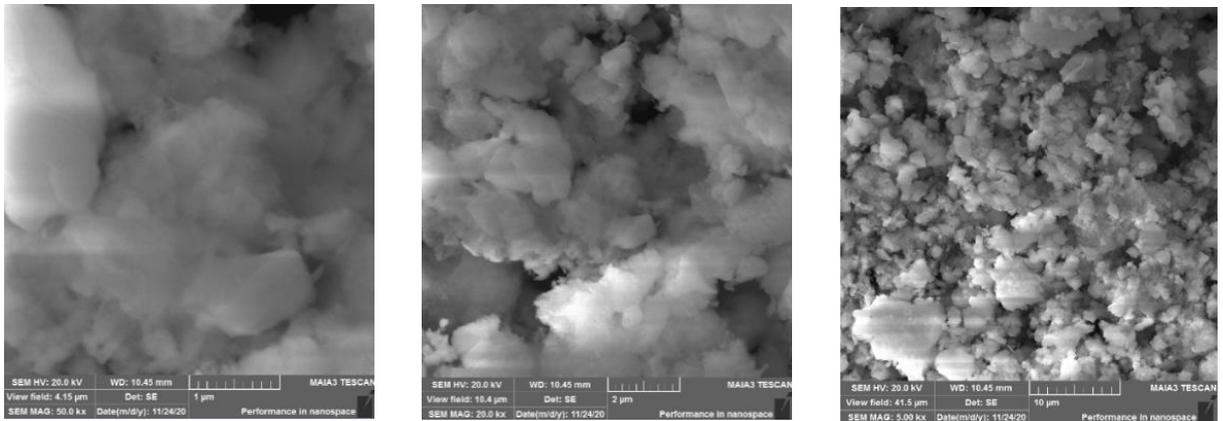
Figure 3.1: SEM of Limestone

The SEM image of limestone shows that is irregular in shape and particles are smaller as compared to clay therefore it will act as a filler and will provide better packing.[38]

EDX of Limestone

Energy Dispersive Xray Spectroscopy (EDX) was performed to analyze the elemental composition of the samples.
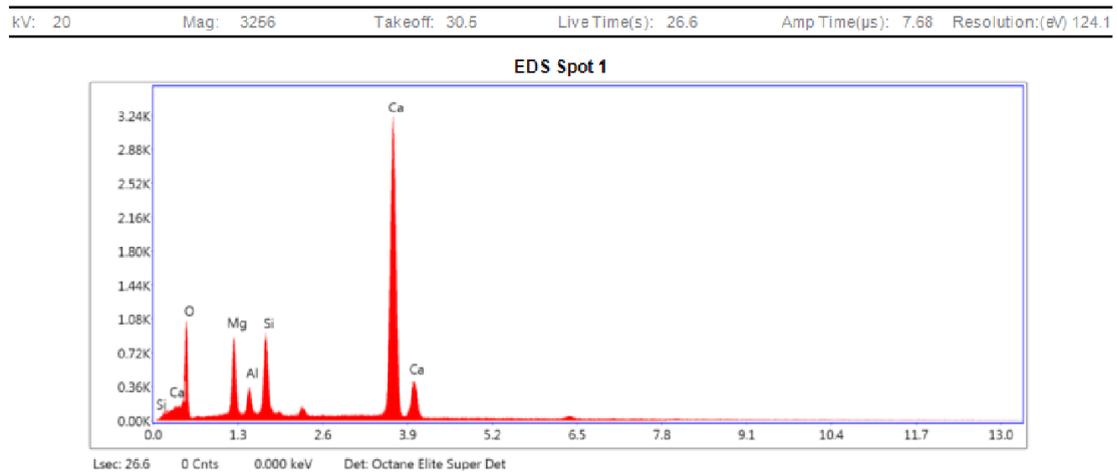
Figure 3.2: EDX of Limestone

Table 3.3: EDX of Limestone

eZAF Smart Quant Results

Element	Weight %	Atomic %	Net Int.	Error %	Kratio	Z	R	A	F
O K	40.71	60.06	469.97	10.77	0.0528	1.0743	0.9522	0.1208	1.0000
MgK	7.56	7.34	420.58	8.01	0.0330	0.9953	0.9880	0.4353	1.0069
AlK	2.08	1.82	133.13	9.43	0.0105	0.9589	0.9956	0.5216	1.0116
SiK	6.17	5.19	476.00	6.42	0.0394	0.9804	1.0028	0.6411	1.0156
CaK	43.47	25.60	2519.67	1.85	0.3989	0.9274	1.0387	0.9795	1.0106

The EDX results of limestone show maximum presence of calcium and oxygen which are its main components. It also shows trace amounts of other elements too.

3.1.4 Water

The water used in the preparation of the mixes was potable drinking tap water.

3.2   Clay Characterization

3.2.1 SEM

SEM of Clay Site A
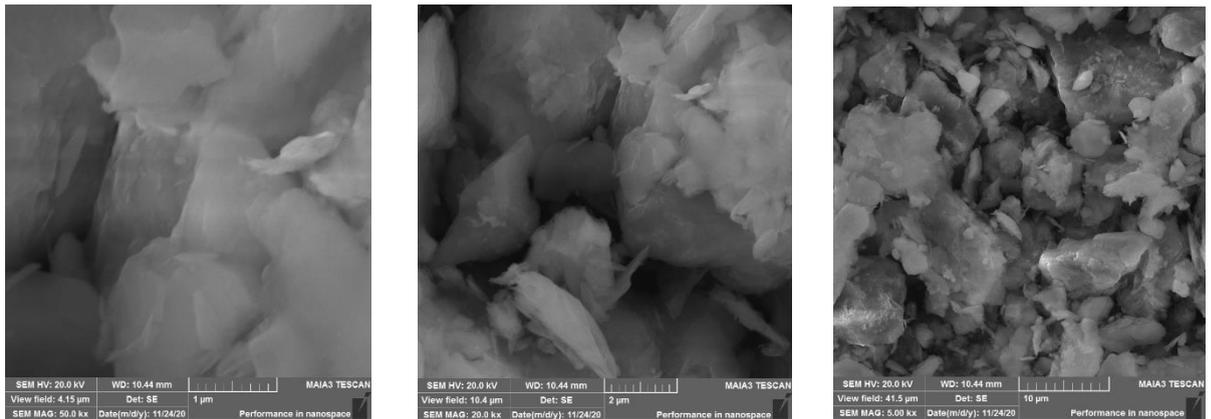
Figure 3.3: SEM of Clay Site A

The SEM images of clay A shows that the particles are sharp edges and are dense which will decrease the workability of the mix[39]

SEM of Clay Site B
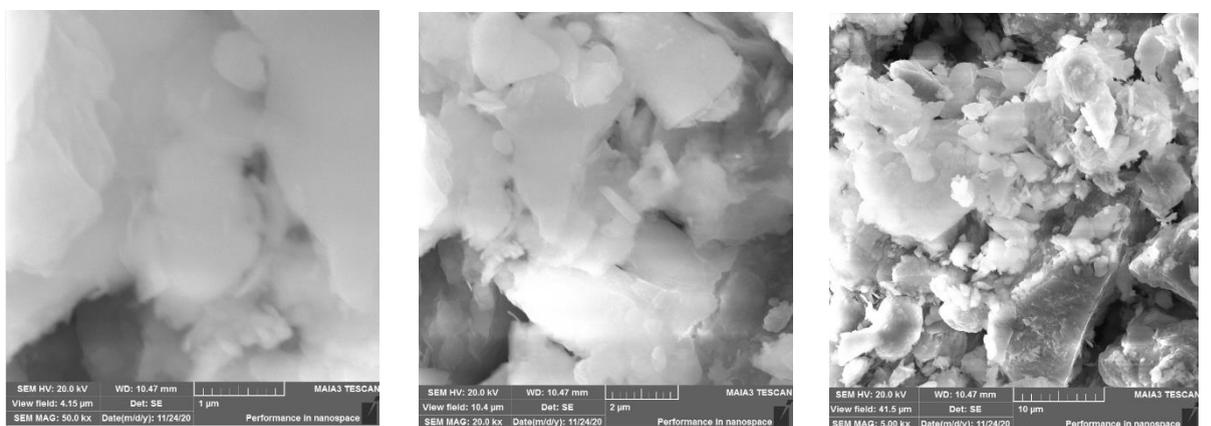
Figure 3.4: SEM of Clay Site B

The SEM images show that sample B has some rounded and pointed extensions which will enhance workability and packing ability.[38]

SEM of Clay Site C
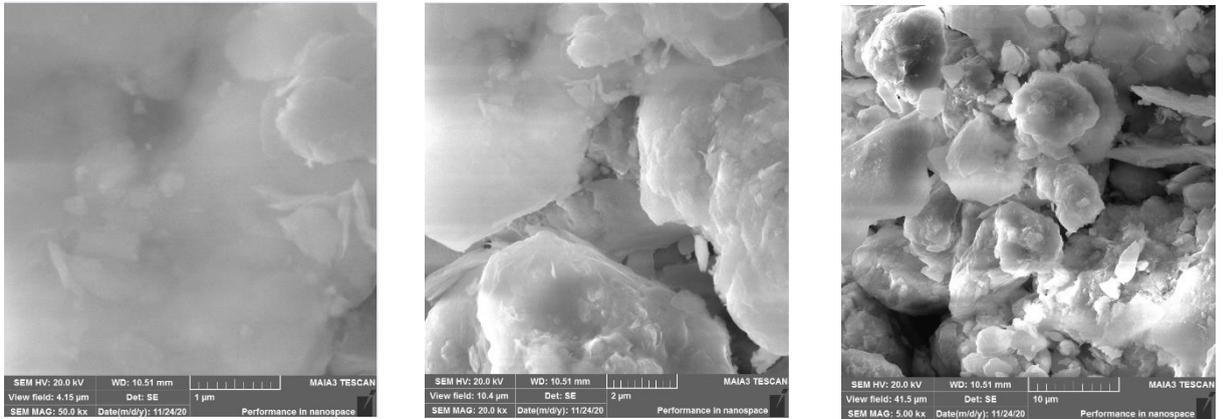
Figure 3.5: SEM of Clay Site C

The SEM images show that the particles of sample C have rounded extensions which may increase workability but will also increase voids due to poor packing.[40]

3.2.2 EDX

Clay Site A

Table 3.4: EDX of Clay Sample A

eZAF Smart Quant Results

Element	Weight %	Atomic %	Net Int.	Error %	Kratio	Z	R	A	F
O K	39.89	54.96	654.43	9.15	0.1127	1.0658	0.9655	0.2850	1.0000
NaK	1.92	1.84	46.43	13.99	0.0069	0.9694	0.9922	0.3665	1.0071
AlK	11.22	9.17	598.31	5.44	0.0724	0.9501	1.0073	0.6677	1.0175
SiK	37.49	29.43	1941.72	4.73	0.2461	0.9712	1.0142	0.6736	1.0035
K K	1.35	0.76	53.38	12.68	0.0107	0.9011	1.0433	0.8594	1.0260
CaK	4.09	2.25	141.98	8.98	0.0344	0.9176	1.0481	0.8978	1.0227
FeK	4.04	1.60	74.06	12.72	0.0354	0.8186	1.0693	0.9946	1.0759
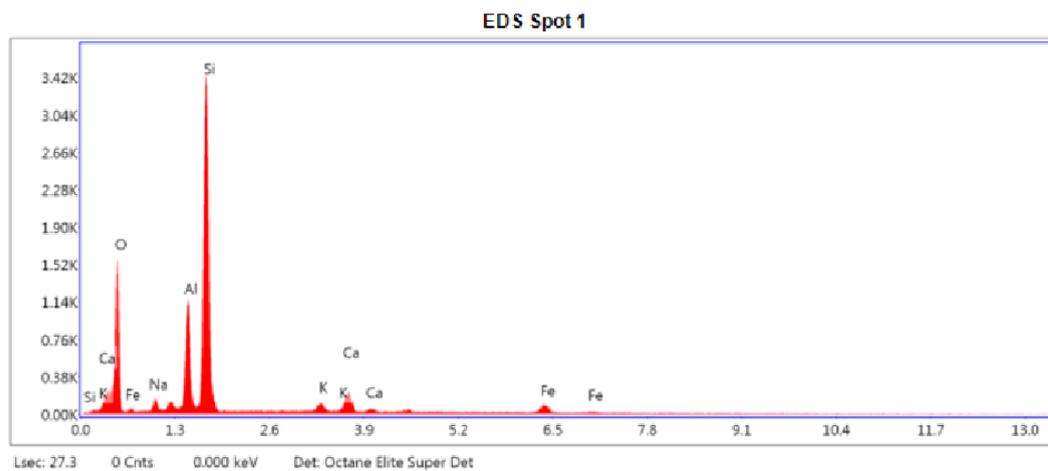
Figure 3.6: EDX of Clay sample A

The EDX results of clay sample A show maximum amounts of aluminum and silica which confirms presence of metakaolin.

Clay Site B

Table 3.5: EDX of Clay Sample B

eZAF Smart Quant Results

Element	Weight %	Atomic %	Net Int.	Error %	Kratio	Z	R	A	F
O K	36.62	55.47	256.43	10.75	0.0602	1.0851	0.9503	0.1514	1.0000
MgK	0.73	0.72	19.82	23.84	0.0032	1.0055	0.9863	0.4416	1.0087
AlK	6.51	5.84	227.13	7.35	0.0375	0.9688	0.9939	0.5875	1.0126
SiK	19.43	16.76	739.94	5.34	0.1279	0.9905	1.0012	0.6589	1.0086
K K	8.71	5.40	281.56	4.81	0.0773	0.9200	1.0321	0.9137	1.0553
CaK	21.32	12.89	555.36	3.46	0.1837	0.9370	1.0373	0.9040	1.0172
FeK	6.70	2.91	87.97	9.92	0.0574	0.8369	1.0609	0.9719	1.0534
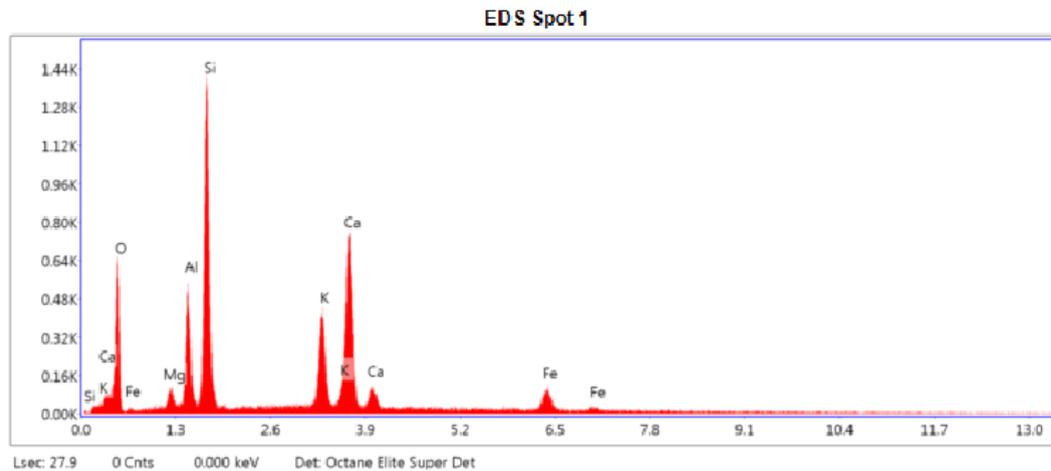
Figure 3.7: EDX of Clay sample B

The EDX results of clay sample B also shows a large amount of aluminum and silica which confirms presence of metakaolin.

Clay Site C

Table 3.6: EDX of Clay Sample C

eZAF Smart Quant Results

Element	Weight %	Atomic %	Net Int.	Error %	Kratio	Z	R	A	F
B K	36.69	52.26	143.64	10.94	0.0838	1.0250	0.9584	0.2230	1.0000
O K	37.40	36.00	1233.34	9.68	0.0704	1.0312	0.9907	0.1826	1.0000
NaK	0.84	0.57	57.54	13.33	0.0028	0.9366	1.0152	0.3558	1.0038
MgK	1.10	0.70	136.42	8.97	0.0054	0.9526	1.0222	0.5171	1.0066
AlK	2.87	1.64	437.24	5.87	0.0176	0.9173	1.0287	0.6617	1.0097
SiK	5.53	3.03	939.96	4.27	0.0395	0.9374	1.0349	0.7558	1.0102
CaK	14.01	5.38	1580.78	1.92	0.1273	0.8849	1.0648	1.0073	1.0195
FeK	1.57	0.43	84.84	10.80	0.0135	0.7889	1.0820	1.0043	1.0818
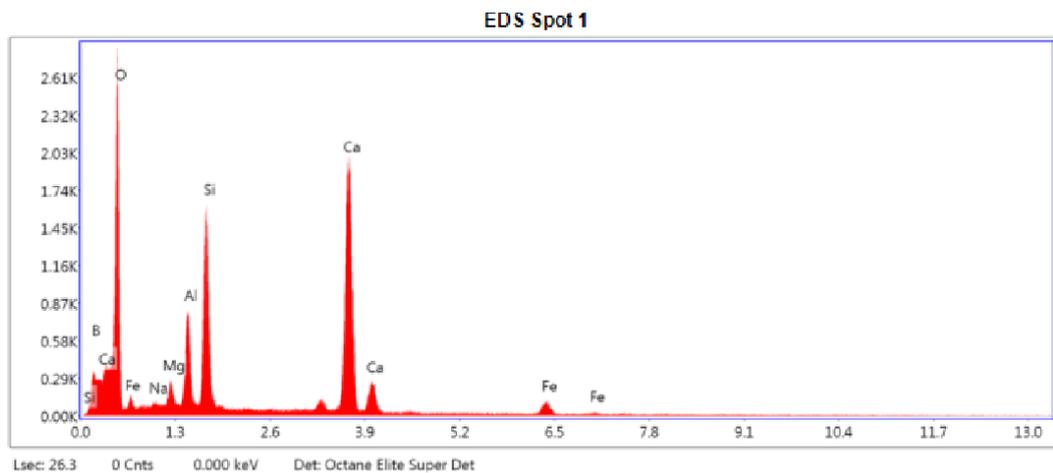
Figure 3.8: EDX of Clay sample C

The EDX results of clay sample C shows less amounts of aluminum and silica hence it will have less metakaolin.

3.2.3 XRF

X-ray florescence technique (XRF) is used to measure the chemical composition of clay types used to prepare the LC^3 binder systems.

Table 3.7: XRF of Clay Sites A, B, and C

Chemical Composition	Clay Site-A	Clay Site-B	Clay Site-C
SiO₂ %	57.07	56.07	33.20
Al₂O₃ %	12.68	14.68	7.89
Fe₂O₃ %	4.08	5.18	4.89
CaO %	8.26	9.36	39.48
MgO %	2.12	2.72	2.44
K₂O %	1.98	2.06	2.07
Na₂O %	0.81	0.92	1.10
SO₃ %	0.01	0.01	0.02
Cl %	0.001	0.000	0.011
Sum of Al₂O₃. SiO₂ and Fe₂O₃	73.83	75.93	45.98

According to ASTM C-618, Clay A and B meet the minimum requirement of 70% for $SiO_2+Al_2O_3+Fe_2O_3$ which is required for cement replacements.[3] Clay C does not meet the criteria therefore it is discarded. The SiO_2/ Al_2O_3 molecular ratio for Clay A, B and C is 4.5, 3.8 and 4.2 respectively which is higher as compared to the ratio for kaolinite ($SiO_2/ Al_2O_3 =2$) indicating huge quartz content[41]. [3]

3.2.4 TGA

Thermogravimetric analysis, also known as TGA, is a technique used to determine the amount of a certain compound in each sample depending upon the mass loss at given temperature. This method was used to determine the amount of kaolinite ($Al_2O_3 2SiO_2 \cdot 2H_2O$) present in the clay. The hydroxylation of kaolin occurs at temperature $400^oC – 600^oC$ [42]. So, at this temperature the mass loss of all the three clay samples

was noted and this mass loss at calcination is used to determine the kaolinite content with the help of Equation 1:

$$\text{Wt\% kaolinite} = \frac{Wt_{400} - Wt_{600}}{Wt_{200} - Wt_i} \times 7.17 \times 100$$

Where Wt_{400} is the weight of sample at 400ºC, similarly Wt_{600} is the weight at 600 ºC, Wt_{200} is the weight of sample at 200 ºC and Wt_i is the initial weight of the sample. The 7.17 in the equation is actually the ratio of molar mass of kaolinite to the molar mass of 2 moles of water since there are 2 molecules of water of crystallization attached to the one molecule of kaolinite.

With the help of TGA results the kaolinite content of the three clay samples is given below

Table 3.8: %Kaolinite of Clay Sites A, B, and C

A Before Calcination		B Before Calcination		C Before Calcination	
% Kaolinite	20.37%	% Kaolinite	25.67%	% Kaolinite	18.48%

The clay from site B was selected in this research due to higher content of kaolinite.

3.2.5 XRD

Xray diffraction is a technique used to find the crystallographic makeup of a sample. For this test, a small sample was extracted and analyzed.
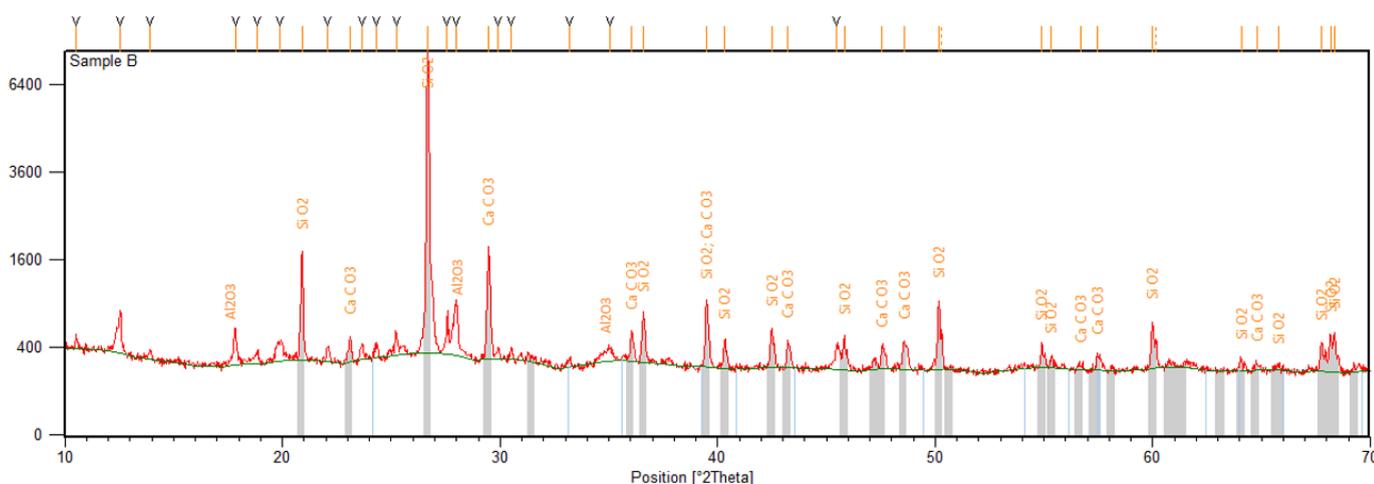
Figure 3.9: XRD of Clay Site B

XRD peaks show quartz and aluminum oxide mineral, ensuring the presence of metakaolin in the clay sample. Quartz has a hexagonal structure, SiO_2 has a tetrahedral arrangement and Al_2O_3 has a hexagonal lattice.

3.3 Formulations and Mix Designs

Total including ten formulations including OPC (control) were designed against water to binder ratio of 0.4. The mix proportions were calculated by mass and are presented in the following table.

Table 3.9: Formulations and mix designs (calculated per kg)

	Cement (g)	Water (g)	Calcined Clay (g)	Limestone (g)
OPC	714.286	285.714	-	-
LC³-30 2:1	500.000	285.714	142.857	71.429
LC³-50 2:1	357.143	285.714	238.095	119.048
LC³-80 2:1	142.857	285.714	380.952	190.476
LC³-30 1:1	500.000	285.714	107.143	107.143
LC³-50 1:1	357.143	285.714	178.571	178.571
LC³-80 1:1	142.857	285.714	285.714	285.714
LC³-30 3:1	500.000	285.714	160.714	53.571
LC³-50 3:1	357.143	285.714	267.857	89.286
LC³-80 3:1	142.857	285.714	428.571	142.857

The test matrix indicating the type of test and the total formulation count is given in the table 3.9.

Table 3.10: Casting Scheme

	Days	Formulations	No. of Samples	Total
Compressive Strength	1	10	3	30
	7	10	3	30
	21	10	3	30
	28	10	3	30
Flexure strength	28	10	2	20
Total				**140**

Grout was mixed using the standard procedure from ASTM C 778, which is used for mixing hydraulic cement paste and mortar. Materials were weighed and added. Table 3.11 explains the procedure of grout preparation.

Table 3.11: Procedure for grout preparation

Step 1	The materials were weighed as per the mix design. Hobart mixture was used for mix preparation
Step 2	Materials were placed in the bowl
Step 3	Water was added according to the mix design of formulations and allowed 30 sec for absorption
Step 4	Hobart mixture was started at slow speed for 30 sec
Step 5	Mixture was stopped for 15 sec to scrap down any grout stuck on sides
Step 6	Mixture was started at fast speed and mixed for 60 sec

After preparation of grout, cubes and prism molds were casted. For compressive strength test, 3 mortar cubes were casted for each of the 10 formulations to be tested on days 1,7, 21 and 28 days. For flexure strength test, 2 prisms were casted for each of the 10 formulations to be tested on 28th day. This makes a total of 140 samples for one clay site.
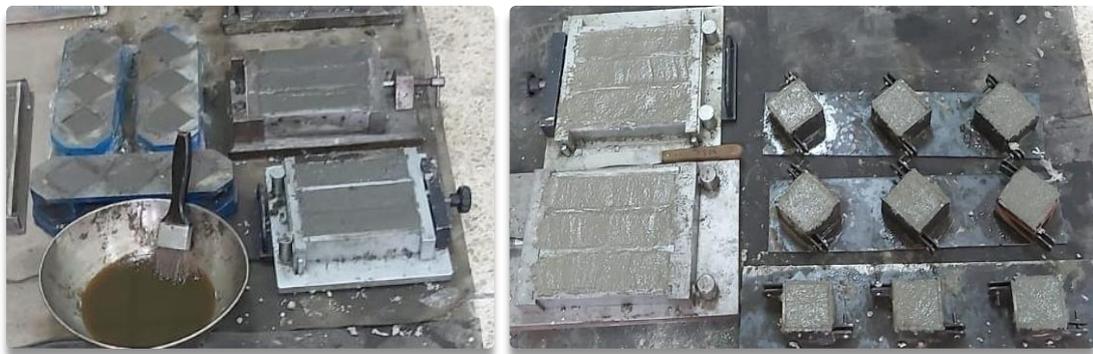
Figure 3.10: Mortar cubes and prisms

3.4 Curing

After 24 hours, the samples were demolded, marked for identification purposes, and immersed in water contained in a curing tank at room

temperature and pressure. The samples were removed one day before test and air dried to ensure dry surface during testing.

3.5 Test Procedure

3.5.1 IST and FST

To study the initial and final setting time of our LC^3 formulations, ASTM C-191 was used. The procedure followed was as below:

- A binder paste was made consisting of the material percentages of respective formulation

- The vicat mould was filled completely and the surface was smoothed.

- The mould was placed under the rod of vicat apparatus having a needle attached to the rod.

- The rod's height was adjusted as the height of the mould with the help of screws, just as the needle touched the surface.

- The needle was dropped and the value of penetration was noted.

- This process was repeated until the penetration value is about 5±1 mm from the bottom surface.

- The time was noted from the addition of water in the mixture to the penetration value of 5±1 mm from bottom. This value was noted as Initial Setting Time of the blend.

- After this the needle was replaced by another needle with a ring around its pointy end.

- And then it was dropped from the surface height of the vicat mould.

- This was done until there was no impression of the ring was imprinted on the surface of the mix, but only a needle dot.

- Time till this stage was noted as the final setting time of the blend.

    .

RESULTS AND DISCUSSION

4.1 IST and FST

To study the initial and final setting time of our LC^3 formulations, ASTM C-191 was used.

The results of the initial and final setting time of the four formulations OPC, LC^3-30, LC^3-50, and LC^3-80 are represented in the graph below:
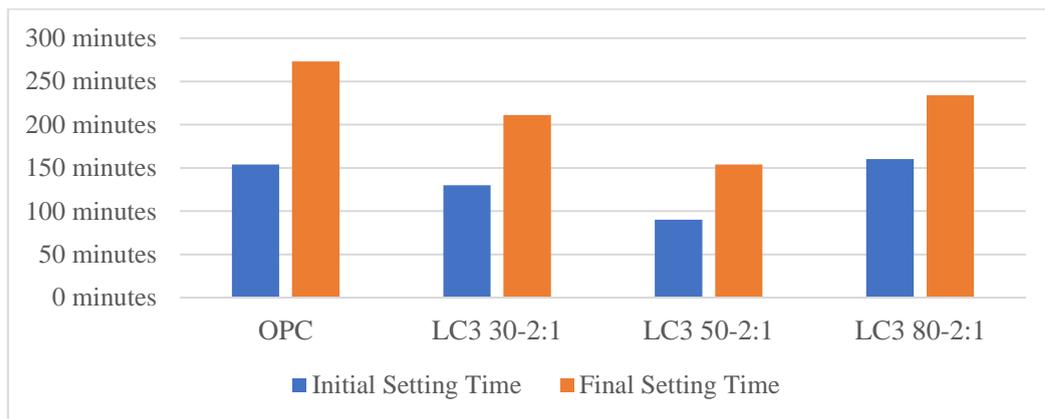
Figure 4.1: IST and FST

With increase in replacements the initial and final setting time for w/c ratio of 0.4 decreases but it then increases for LC^3 80 as the percentage of cement is very less in the mix

4.2 Compressive Strength

The compressive strength of the LC^3 mixes was tested in accordance with the ASTM C109. Mortar cubes of the scheme given in the table. 3 cubes were casted to be tested on 1, 7, 21 and 28 days. The samples were submerged in water, confirming 100% humidity, and were removed from water 24 hours before testing to let the samples air dry. The compressive strength of the cubes is given in the figures below:
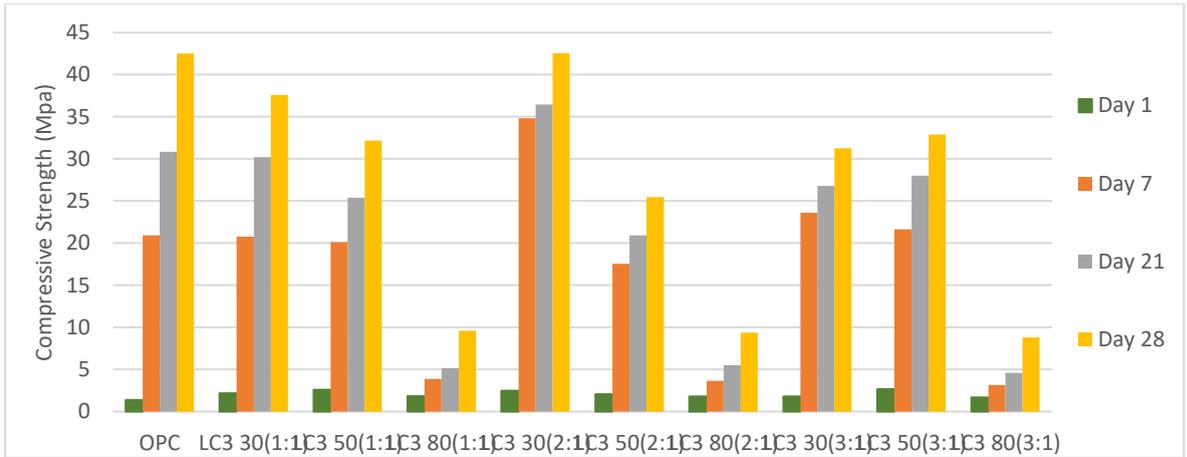
Figure 4.2: Compressive strengths of OPC, LC^3-30, LC^3-50, LC^3-80

It can be seen from the figures that LC^3 mixes reach most of their strength at around day 7. LC^3 -30 (2:1) showed better results as compared to other mixes. LC^3 -80 (3:1) having most of the replacement material showed the least strength.

The presence of calcined clay accelerates the initial hydration phase due to its filler nature and presence of more nucleation sites. Therefore, the early strength of LC^3 systems is higher than that of OPC.[3]
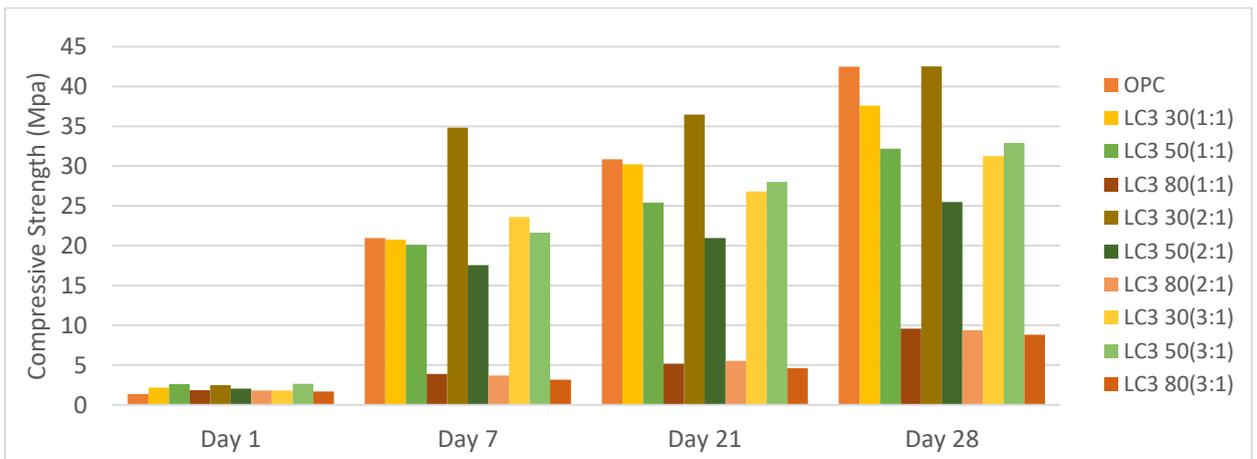
Figure 4.3: Comparative Compressive strengths of OPC, LC^3-30, LC^3-50, LC^3-8

The following figure it can be said that within the LC^3 systems the mix having highest clinker amount exhibits highest compressive strength. When compared to OPC the clays being more water absorbing material results in less excess water pores and hence LC^3 mixes yield good strength even at water content of 0.4.[43]

4.3   Flexure Strength

Flexure strength of the LC^3 systems were determined in accordance with ASTM C-348. Prisms were casted for LC^3 with clay to limestone ratio 2:1 and OPC. Each was tested on day 28. The results are given in the figure below:
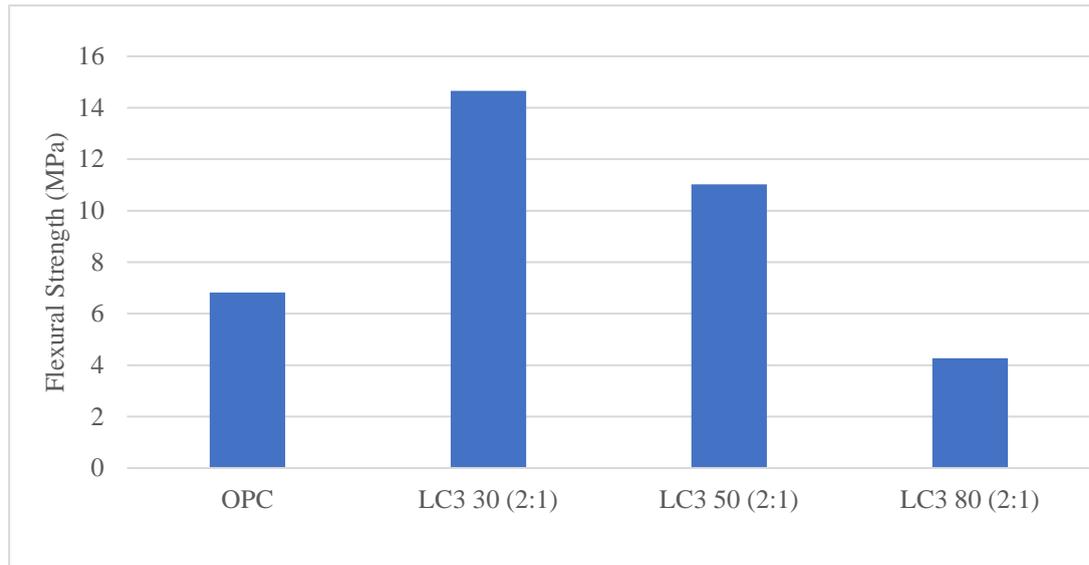
Figure 4.4: Flexure strengths of OPC, LC^3-30, LC^3-50, LC^3-80

It can be seen from the figure that the LC^3 mixes show higher flexural strength as compared to OPC. That can be related to the fact that with the incorporation of calcined clay the ductility of the mix increases[20].

4.4   Carbon Footprint and Energy Consumption

The production of concrete has a huge impact on the environment as it amounts for 5-8% of the total CO_2 emissions of the world produced by humans.[44] Of this figure, 95% CO_2 is emitted during the production process of clinker, making cement production the second largest emitter of human produced CO_2 after power generation.[45] Furthermore, cement is the most consumed product after water and increasing urbanization can increase this demand[46] which will further increase the emission of anthropogenic CO_2 and this is an alarming situation for us.

Carbon footprint is the total amount of carbon dioxide produced from

a certain action. One of our main aims was the reduction of carbon dioxide emissions from cement production by replacing a percentage of clinker in the mix. To determine the amount of CO_2 reduction, carbon footprint and energy consumptions of all the materials used was extracted from literature.

Clay can be calcined using three different ways: by a clinker kiln, a refurbished kiln, and a flash calciner. Using the literature data, all three processes are compared. The data indicates that refurbishing a kiln for the process of calcination reduces the amount of CO_2 emissions and energy consumption by 58% and 31% respectively.[47] As compared with a flash clinker, the increase in energy for a refurbished kiln is 12% and the rise in CO_2 production is only 21%.[1] In terms of expenditure, a flash clinker has a capital cost of $US 24/ton where as refurbishing a kiln has a capital cost in the range of $US 12/ton.[48] Another aspect that has to be noted is that refurbishing an old cement plant is much faster than installing a new flash clinker, taking just around 6-8 months instead of 18 months taken for a flash clinker.[1]

Refurbishing an old kiln is also a sustainable alternative as most cement plants have an old and outdated kiln which is used when demands get too high for normal production or when the company faces some gaps in production.[1] Therefore the values of a refurbished kiln will be used in our calculations. The values for limestone powder aren't taken as it isn't heated and hence will not contribute to the CO_2 emissions.[1]

Table 4.1 : Amount of CO_2 produced and Energy used for cement and calcined clay.[1], [49]

Material		kg CO_2 emitted per ton	Energy Used per ton(MJ)
Cement		871	4197
Calcined clay	Kiln (Industrial Trial)	393	4234
	Refurbished kiln	249	3088
	Flash calciner	196	2734

The carbon footprint of each blend is calculated by adding the values of CO_2 emitted in the proportions that the blends are made in. For example, the formula for the carbon footprint of LC^3-30(2:1) will be:

$$Kg\ CO_2\ emitted\ per\ ton\ of\ LC^3 - 30(2:1)$$
$$= 0.7(kg\ CO_2\ emitted\ per\ ton\ of\ cement)$$
$$+ 0.3(\frac{2}{3} \times kg\ CO_2\ emitted\ per\ ton\ of\ calcined\ clay)$$

The same formula and methodology are applied to the calculations of energy consumptions. As seen from the table and graphs attached, increasing the amount of substitution decreases the production of CO_2 and decreases the energy consumption. It is also noted from the graphs the increasing the amount of limestone in the blend also decreases the CO_2 emissions, but the difference is minute, from 26% to 24% for LC^3-30, as the amount of limestone does not change by a large amount. Similar patterns are observed in the energy consumptions as well.

Table 4.2: Carbon Footprint and Energy emission for blends

Material	kg CO_2 emitted per tonne	Percentage difference Of CO_2 emitted w.r.t cement	Energy Used per tonne(MJ)	Percentage difference of energy consumed w.r.t cement
OPC	871	0%	4197	0%
LC^3 30 (1:1)	647	26%	3401	19%
LC^3 30 (2:1)	660	24%	3556	15%
LC^3 30 (3:1)	666	24%	3633	13%
LC^3 50 (1:1)	498	43%	2871	32%
LC^3 50 (2:1)	519	40%	3128	25%
LC^3 50 (3:1)	529	39%	3257	22%
LC^3 80 (1:1)	274	69%	2075	51%
LC^3 80 (2:1)	307	65%	2486	41%
LC^3 80 (3:1)	324	63%	2692	36%
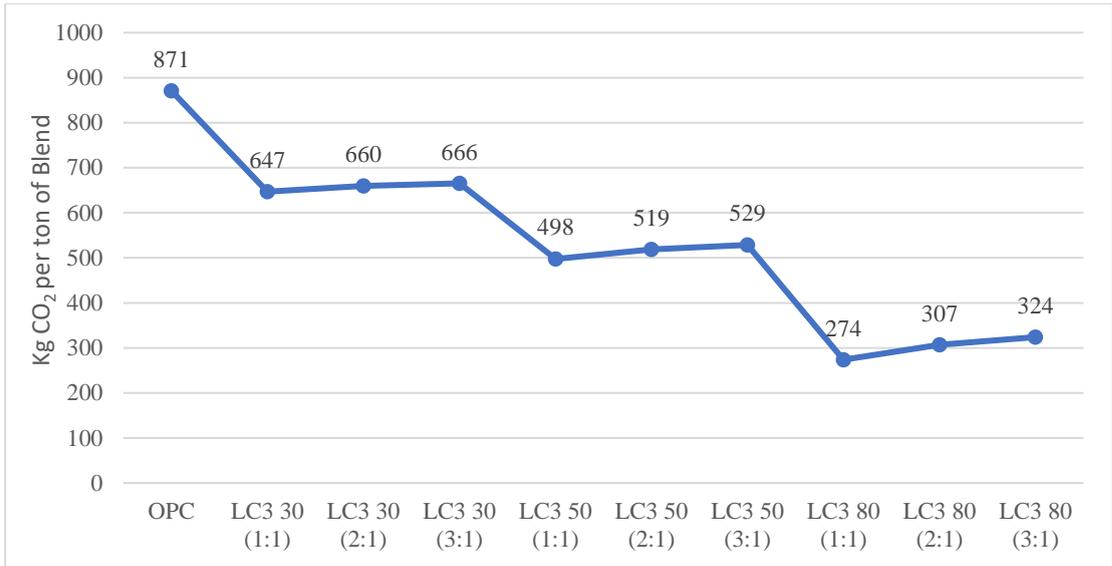
Figure 4.5: kg CO_2 emitted per ton of blend
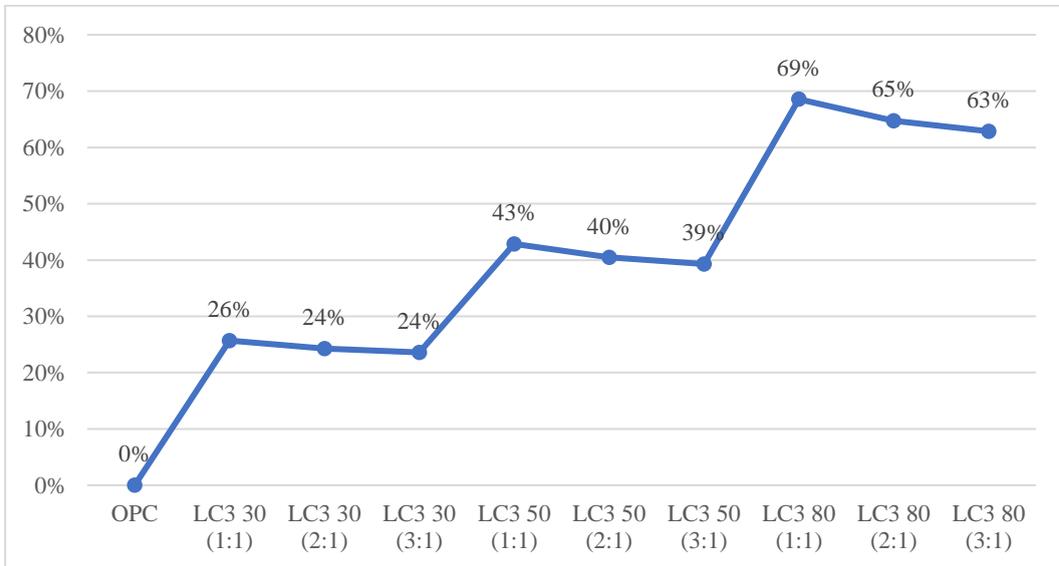
Figure 4.6: Percentage difference Of kg CO_2 emitted per ton w.r.t cement
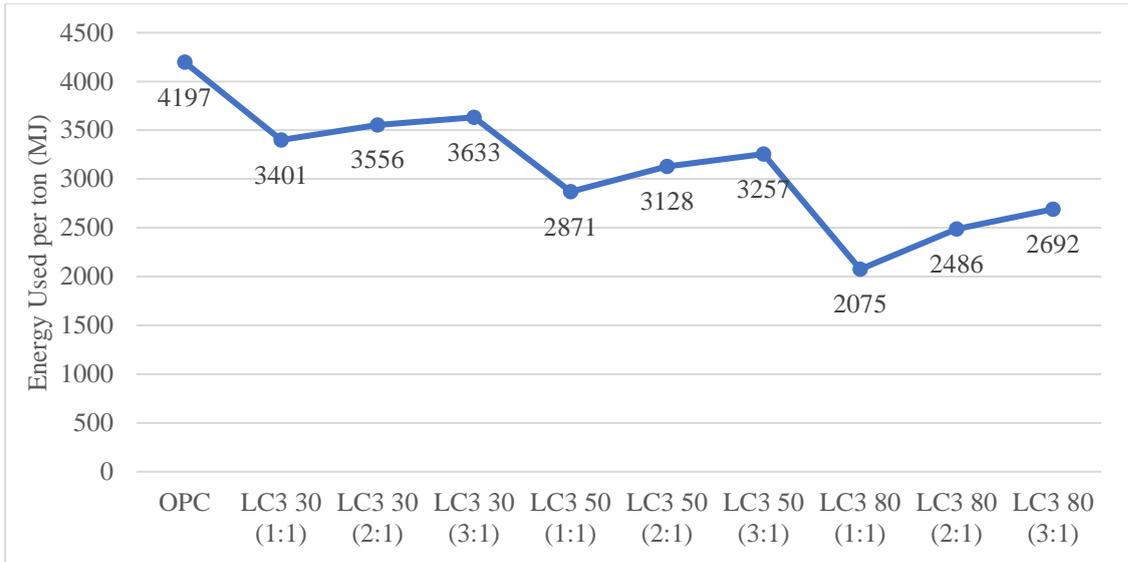
Figure 4.7: Energy Used per ton(MJ)
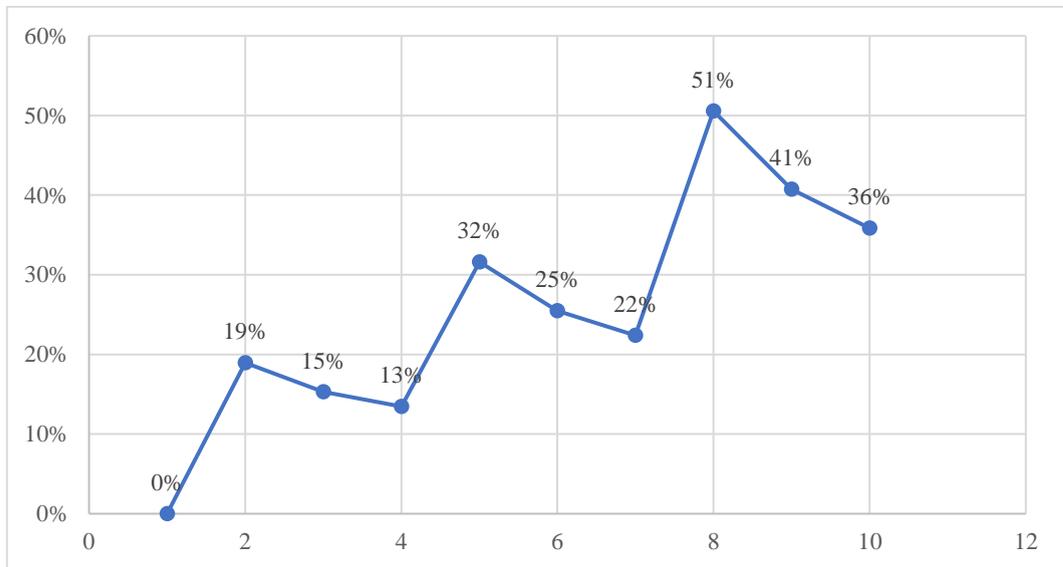
Figure 4.8: Percentage difference of energy consumed per ton w.r.t cement

4.5 Rate of Water Absorption

ASTM D570 Standard test is used to find the relative rate of water absorption by the mortar cubes at 28th day of casting. Weighing balance accurate to 0.1g was used to find the dry and the wet weight of the cubes of different formulations. The result is displayed in the graph below:
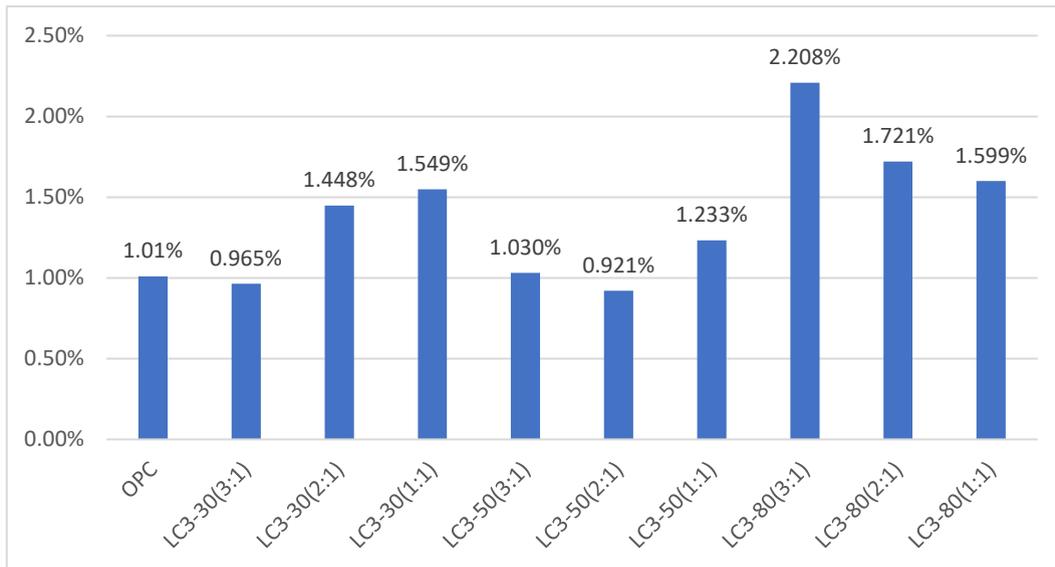
Figure 4.9: Rate of Water Absorption

The graph shows that LC^3-50 (2:1) absorbed the least amount of water indicating that it has the least number of pores. In short, The greater the rate of water absorption the greater the voids present in the specimen at 28th day.

4.6   Microstructure of LC³

4.6.1 SEM

LC³ -30 (1:1)

The SEM images of the sample can indicate presence of metakaolin particles.[50]
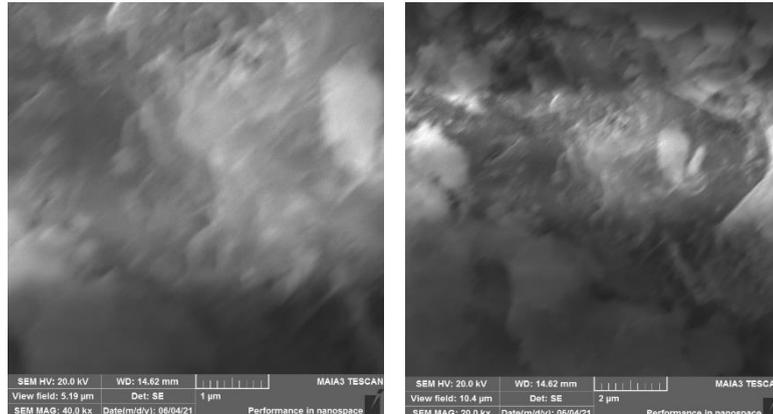
Figure 4.10: SEM of LC³-30 (1:1)

LC³-30(2:1)

The SEM images of the sample indicate presence of metakaolin and calcium carbonate particles.[50]
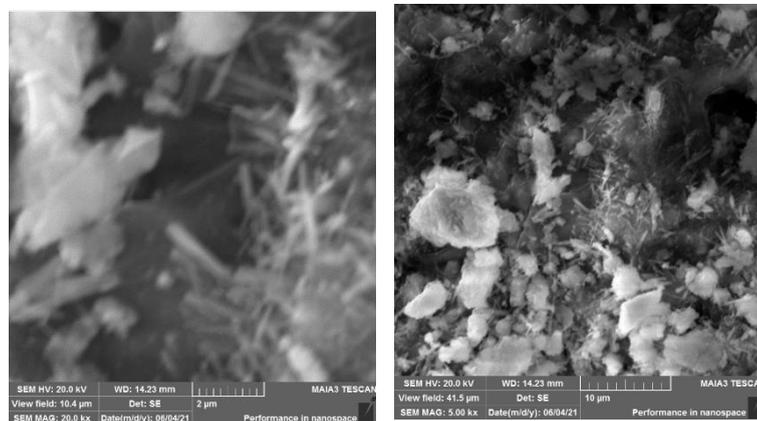
Figure 4.11: SEM of LC³-30 (2:1)

LC³-30(3:1)

The SEM images of the sample indicate presence of metakaolin, calcium carbonate and needle-like particles of ettringite.[1]
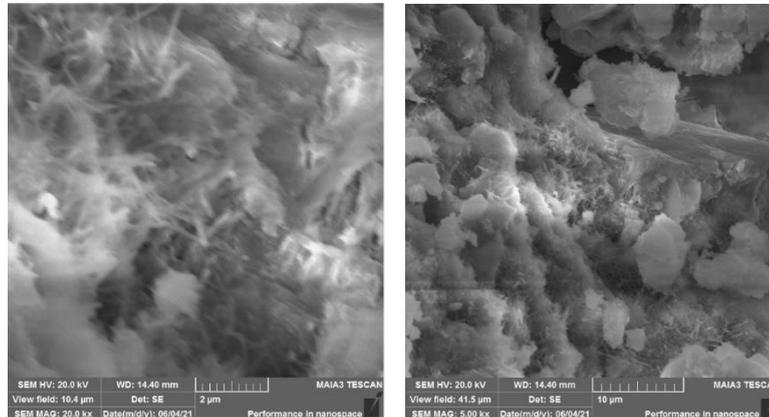
Figure 4.12: SEM of LC³-30 (3:1)

LC³-50(1:1)

The SEM images of the sample indicate presence of metakaolin, calcium carbonate and inner C-S-H particles.[1]
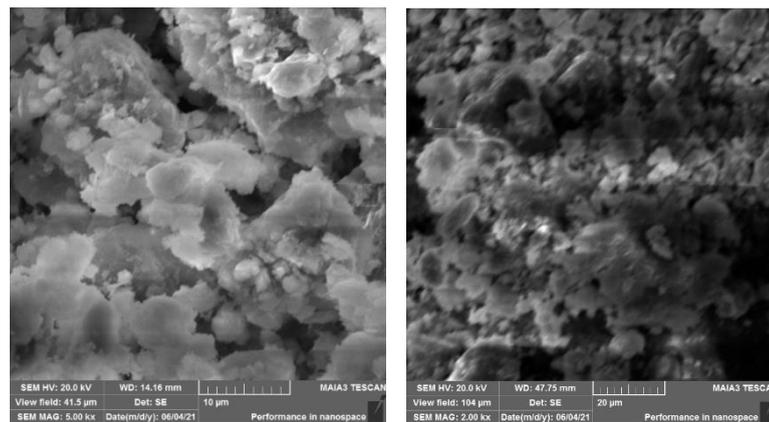
Figure 4.13: SEM of LC³-50 (1:1)

LC³-50(2:1)

The SEM images of the sample indicate presence of metakaolin, calcium carbonate and inner C-S-H particles.[1]
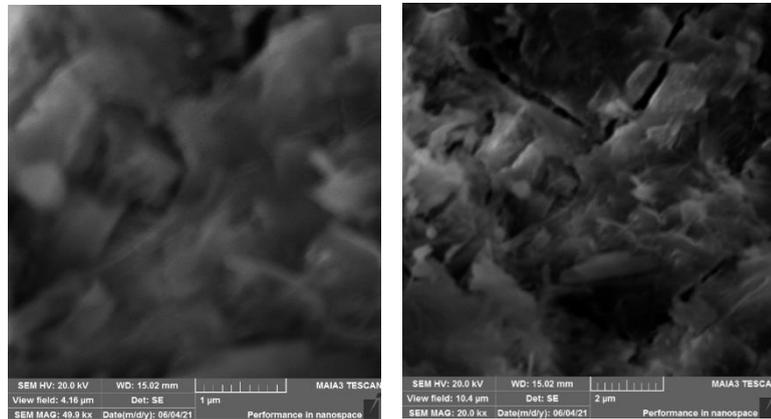
Figure 4.14: SEM of LC³-50 (2:1)

LC³-50(3:1)

The SEM images of the sample can indicate presence of large metakaolin particles.[50]
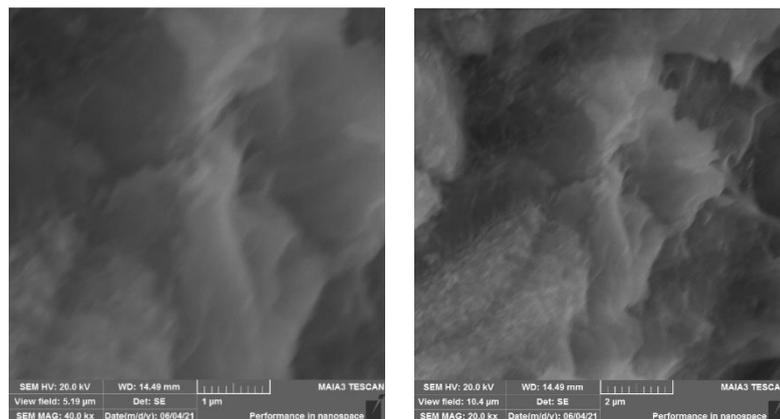
Figure 4.15: SEM of LC³-50 (3:1)

LC³-80(1:1)

The SEM images of the sample can indicate presence of large metakaolin particles and calcium carbonate.[50]
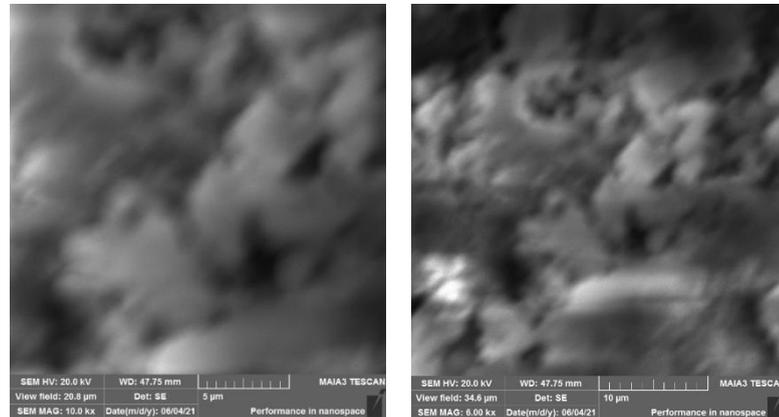
Figure 4.16: SEM of LC³-80 (1:1)

LC³-80(2:1)

The SEM images of the sample indicate presence of metakaolin, calcium carbonate, inner C-S-H and needle-like particles of ettringite.[1]
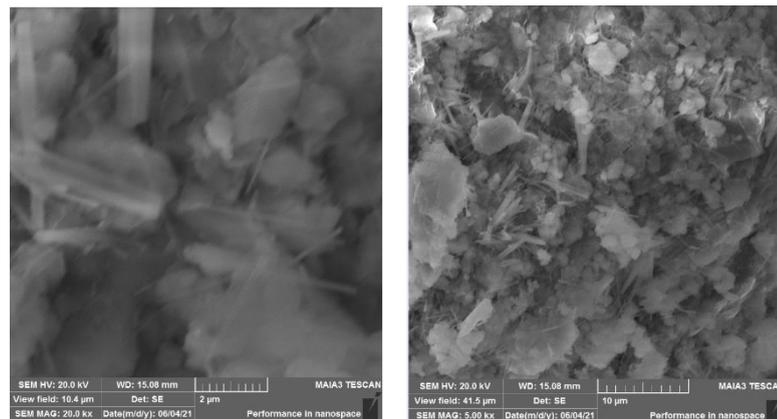
Figure 4.17: SEM of LC³-80 (2:1)

LC^3-80(3:1)

The SEM images of the sample indicate presence of metakaolin, calcium carbonate, inner C-S-H,pertlandite and needle-like particles of ettringite.[1]
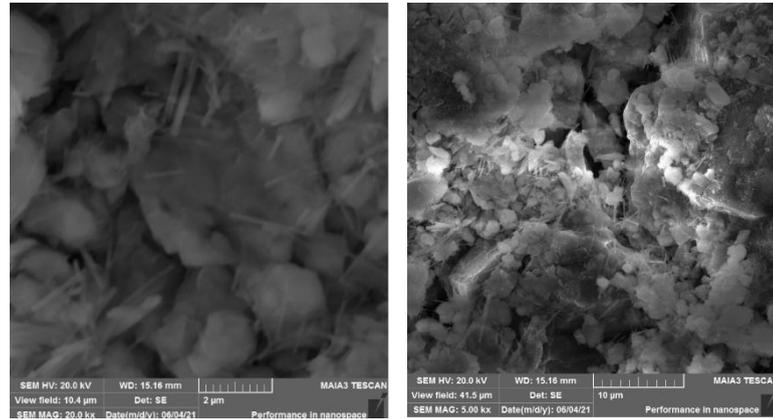
Figure 4.18: SEM of LC^3-80 (3:1)

4.6.2 EDX

LC^3-30(1:1)

The EDX results of LC^3-30(1:1) shows maximum amounts of Calcium with trace amounts of silica.
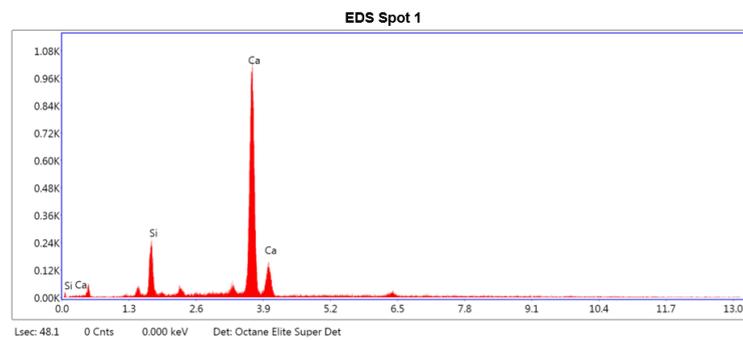
eZAF Smart Quant Results

Element	Weight %	Atomic %	Net Int.	Error %	Kratio	Z	R	A	F
SiK	8.92	12.26	67.86	7.07	0.0696	1.0491	0.9619	0.7257	1.0252
CaK	91.08	87.74	450.80	2.15	0.8981	0.9950	1.0035	0.9831	1.0079

Figure 4.19: EDX of LC^3-30 (1:1)

LC³-30(2:1)

The EDX results of LC³-30(2:1) shows maximum amounts of calcium, oxygen and aluminum with trace amounts of silica, magnesium, Iron and sulphur.

Element	Weight %	Atomic %	Net Int.	Error %	Kratio	Z	R	A	F
O K	48.30	67.32	230.49	10.44	0.0838	1.0671	0.9584	0.1626	1.0000
MgK	1.80	1.65	30.74	11.99	0.0081	0.9882	0.9936	0.4549	1.0074
AlK	7.76	6.41	164.51	6.77	0.0441	0.9520	1.0011	0.5919	1.0096
SiK	4.29	3.41	98.49	7.20	0.0278	0.9733	1.0081	0.6568	1.0133
S K	4.10	2.85	97.20	7.43	0.0330	0.9538	1.0211	0.8195	1.0299
CaK	31.13	17.32	514.48	2.33	0.2817	0.9203	1.0431	0.9699	1.0140
FeK	2.61	1.04	20.44	13.10	0.0222	0.8215	1.0654	0.9762	1.0588

Figure 4.20: EDX of LC³-30 (2:1)

LC³-30(3:1)

The EDX results of LC³-30(3:1) shows maximum amounts of calcium, oxygen and silica with trace amounts of aluminum, magnesium, potassium and sulfur.

Element	Weight %	Atomic %	Net Int.	Error %	Kratio	Z	R	A	F
O K	49.55	68.05	263.06	10.34	0.0826	1.0628	0.9605	0.1569	1.0000
NaK	1.59	1.52	17.09	16.44	0.0048	0.9670	0.9876	0.3095	1.0041
MgK	1.47	1.33	28.93	12.74	0.0066	0.9840	0.9955	0.4545	1.0072
AlK	4.12	3.36	101.14	7.86	0.0235	0.9479	1.0029	0.5943	1.0109
SiK	6.89	5.39	190.85	5.75	0.0466	0.9691	1.0099	0.6892	1.0133
S K	2.82	1.93	77.37	7.71	0.0228	0.9496	1.0228	0.8232	1.0316
K K	1.49	0.84	36.19	12.30	0.0142	0.8995	1.0396	0.9525	1.1126
CaK	32.06	17.58	606.89	2.24	0.2878	0.9161	1.0446	0.9687	1.0118

Figure 4.21: EDX of LC³-30 (3:1)

LC³-50(1:1)

The EDX results of LC³-50(1:1) shows maximum amounts of calcium, oxygen and silica with trace amounts of aluminum and magnesium.

Element	Weight %	Atomic %	Net Int.	Error %	Kratio	Z	R	A	F
O K	52.37	69.55	305.85	10.08	0.1004	1.0560	0.9651	0.1814	1.0000
MgK	3.90	3.40	76.34	9.21	0.0182	0.9774	0.9996	0.4753	1.0076
AlK	4.74	3.73	110.66	7.68	0.0268	0.9415	1.0069	0.5928	1.0113
SiK	11.65	8.82	303.99	5.47	0.0774	0.9624	1.0138	0.6824	1.0105
CaK	27.34	14.50	496.37	2.39	0.2450	0.9095	1.0478	0.9725	1.0128
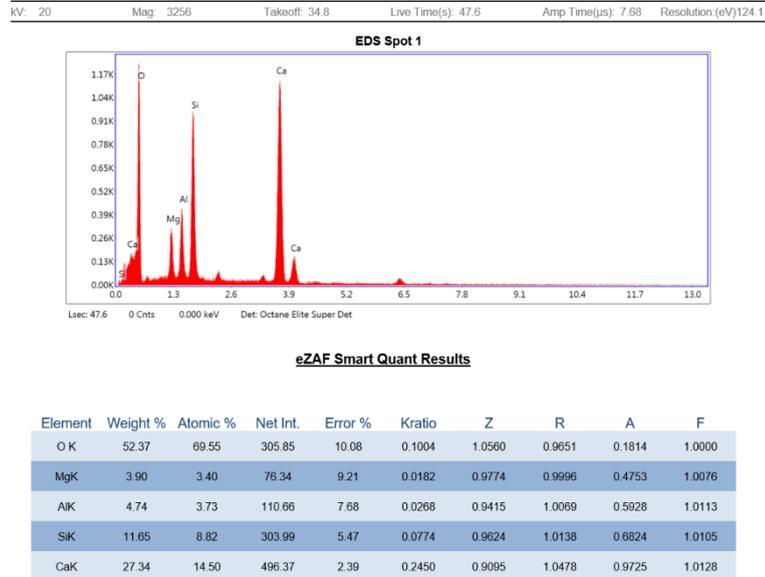
Figure 4.22: EDX of LC³-50 (1:1)

LC³-50(2:1)

The EDX results of LC³-50(2:1) shows maximum amounts of calcium, oxygen, aluminum and silica with trace amounts of magnesium.

Element	Weight %	Atomic %	Net Int.	Error %	Kratio	Z	R	A	F
O K	59.85	76.38	382.81	9.85	0.1228	1.0493	0.9687	0.1955	1.0000
MgK	1.26	1.06	24.03	15.64	0.0057	0.9709	1.0029	0.4585	1.0072
AlK	5.98	4.53	142.56	7.15	0.0340	0.9352	1.0101	0.6020	1.0097
SiK	5.80	4.22	152.17	6.59	0.0382	0.9559	1.0169	0.6809	1.0120
CaK	27.11	13.81	500.94	2.24	0.2447	0.9032	1.0503	0.9862	1.0131

Figure 4.23: EDX of LC³-50 (2:1)

LC³-50(3:1)

The EDX results of LC³-50(3:1) shows maximum amounts of calcium and oxygen with trace amounts of silica.

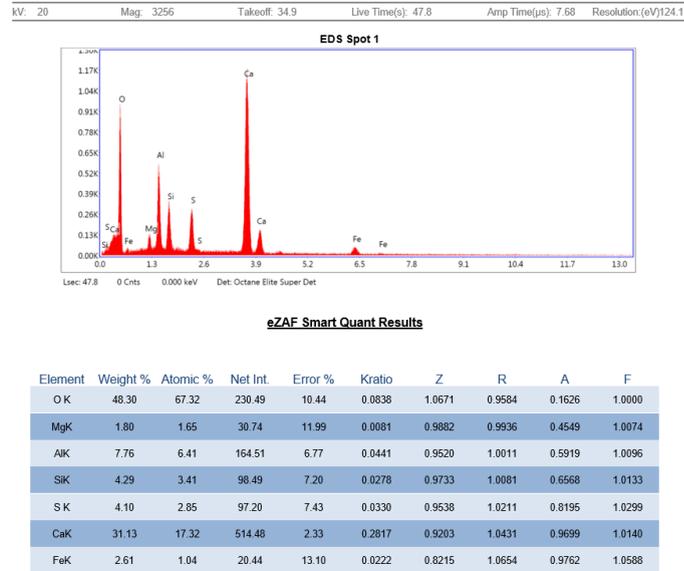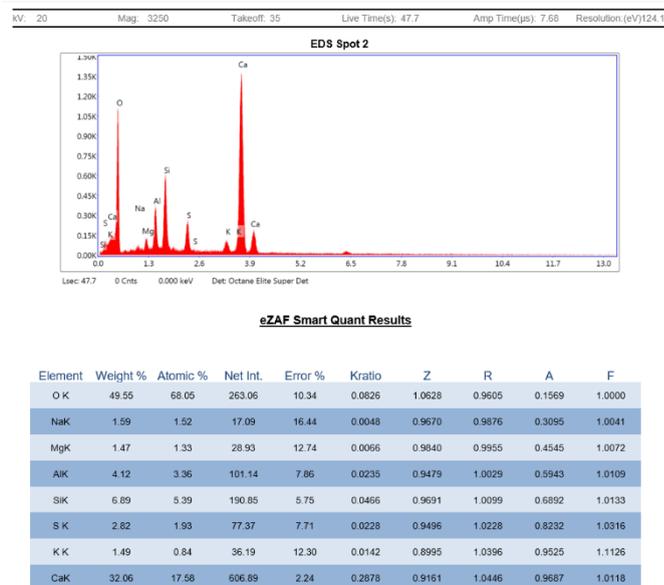| Element	Weight %	Atomic %	Net Int.	Error %	Kratio	Z	R	A	F
O K	23.15	42.38	31.20	13.27	0.0216	1.1082	0.9280	0.0842	1.0000
SiK	4.69	4.89	64.77	7.48	0.0349	1.0137	0.9817	0.7169	1.0243
CaK	72.16	52.73	663.45	1.86	0.6944	0.9604	1.0207	0.9937	1.0086
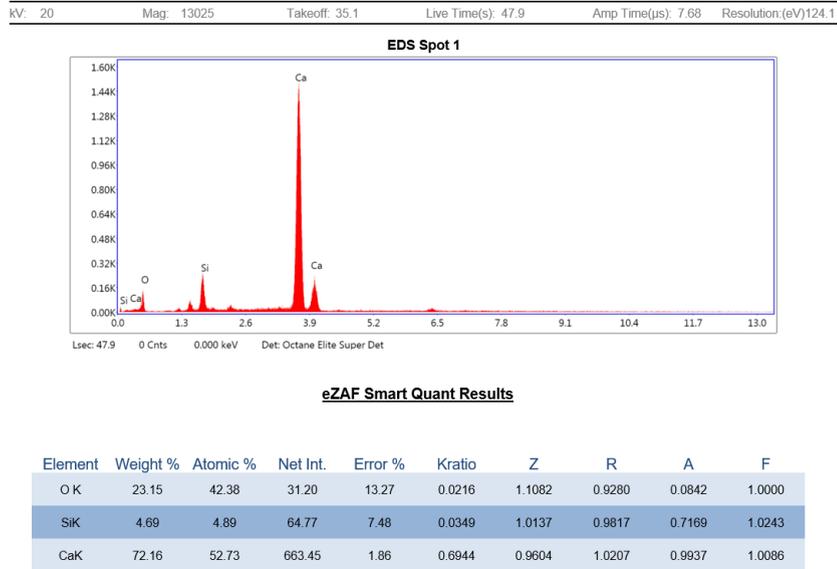
Figure 4.24: EDX of LC³-50 (3:1)

LC³-80(2:1)

The EDX results of LC³-80(2:1) shows maximum amounts of calcium and oxygen with trace amounts of silica, aluminum and magnesium.

Element	Weight %	Atomic %	Net Int.	Error %	Kratio	Z	R	A	F
O K	48.97	66.87	201.54	10.47	0.0850	1.0610	0.9614	0.1636	1.0000
MgK	8.50	7.64	129.52	8.23	0.0401	0.9823	0.9963	0.4771	1.0064
AlK	3.03	2.46	51.29	9.38	0.0161	0.9463	1.0037	0.5553	1.0102
SiK	6.47	5.03	127.30	6.80	0.0421	0.9673	1.0107	0.6640	1.0128
CaK	33.02	18.00	465.87	2.37	0.2994	0.9144	1.0453	0.9802	1.0120
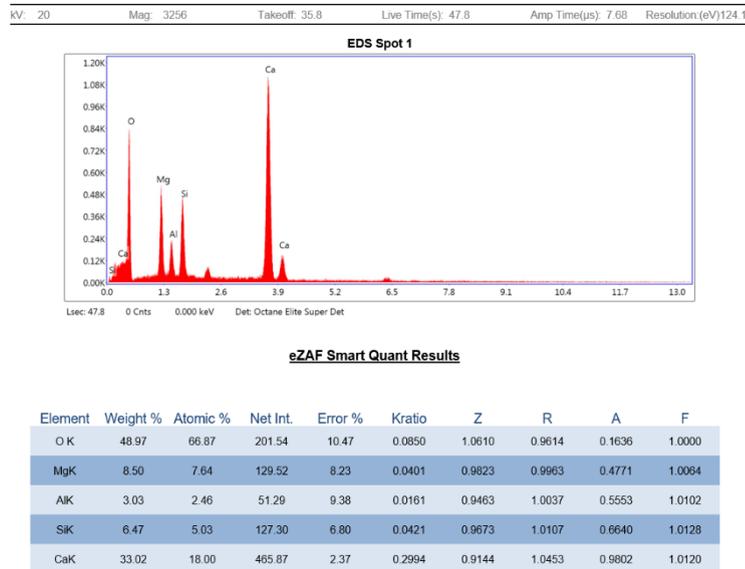
Figure 4.25: EDX of LC³-80 (2:1)

LC³-80(3:1)

The EDX results of LC³-80(3:1) shows maximum amounts of silica and oxygen with trace amounts of aluminum and calcium.

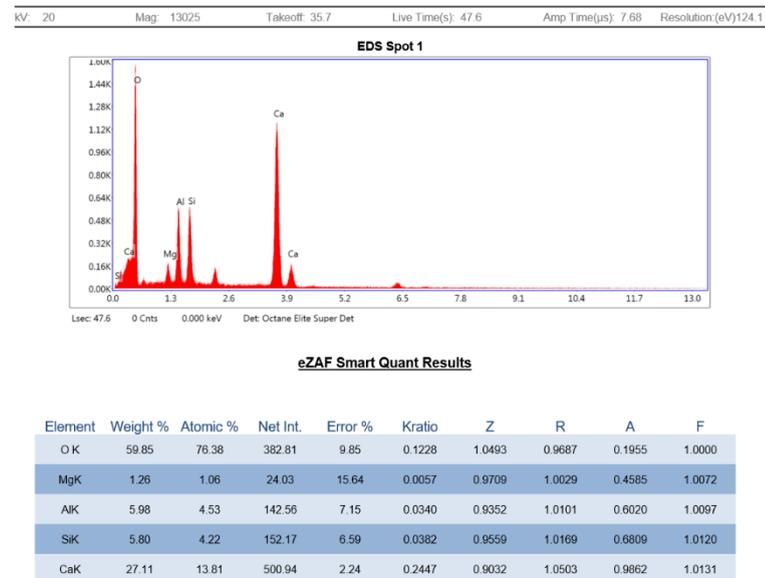**eZAF Smart Quant Results**

Element	Weight %	Atomic %	Net Int.	Error %	Kratio	Z	R	A	F
O K	45.61	60.94	276.48	9.47	0.1183	1.0546	0.9682	0.2460	1.0000
AlK	1.88	1.49	40.45	9.80	0.0129	0.9398	1.0096	0.7102	1.0273
SiK	42.04	31.99	972.68	3.46	0.3265	0.9606	1.0164	0.8050	1.0043
CaK	10.47	5.58	136.73	4.75	0.0893	0.9075	1.0500	0.9250	1.0160

Figure 4.26: EDX of LC³-80 (3:1)

CHAPTER 5

CONCLUSION

Based upon the experiments performed and results obtain, following conclusions can be drawn:

1. The blend of **LC³-30 2:1** (w/b = 0.4) showed the best results for compressive strength. It resulted in the best flexure strength as well. It also reduced the CO_2 emission by 24.3% and the energy consumption by 15.3%

2. Out of the three LC^3 mixes tested, LC^3 80 (2:1) showed the highest decrease in CO_2 emission and energy consumption by 64.8% and 40.8% respectively

3. The blend of **LC³ 50 (2:1)** (w/b=0.4) took the least time to set had the lowest rate of water absorption

4. The increased FST of OPC can be explained by the fact that 0.4 w/c ratio was kept constant for the formulations.

5. Given the anticipated surge in the demand of cement in upcoming years LC^3 can afford us with ample production of the binder system hence fulfilling our future needs

INDUSTRIAL FEASIBILTY AND

FUTURE INVESTMENT

LC^3 binders hold a strong future in cement industry because

- Refurbished cement manufacturing machinery

- Low grade clay - abundantly available

- Economical – energy saver since

(Clinker manufacturing kiln requires a temperature of 1450°C, whilst calcined clay preparation requires 850°C)

RECOMMENDATIONS

1. Comparative study between low- grade and high-grade Clays

2. effect of different types of limestones on the blend

3. utilization of super plasticizers in LC^3 blends

4. effect of different w/b ratios on LC^3 mix

5. durability assessment of different blends of LC^3

REFERENCES

[1]   Y. Cancio Díaz *et al.*, "Limestone calcined clay cement as a low-carbon solution to meet expanding cement demand in emerging economies," *Dev. Eng.*, 2017, doi: 10.1016/j.deveng.2017.06.001.

[2]   P. Markewitz *et al.*, "Carbon capture for CO2 emission reduction in the cement industry in Germany," *Energies*, 2019, doi: 10.3390/en12122432.

[3]   K. Scrivener, F. Martirena, S. Bishnoi, and S. Maity, "Calcined clay limestone cements (LC3)," *Cem. Concr. Res.*, vol. 114, no. November 2017, pp. 49–56, 2018, doi: 10.1016/j.cemconres.2017.08.017.

[4]   C. A. Hendriks, E. Worrell, D. De Jager, K. Blok, and P. Riemer, "Emission Reduction of Greenhouse Gases from the Cement Industry," *Greenh. gas Control Technol. Conf.*, pp. 1–11, 2003.

[5]   M. Antoni, J. Rossen, F. Martirena, and K. Scrivener, "Cement substitution by a combination of metakaolin and limestone," *Cem. Concr. Res.*, vol. 42, no. 12, pp. 1579–1589, Dec. 2012, doi: 10.1016/j.cemconres.2012.09.006.

[6]   B. O. and E. M. Changling Hea, "POZZOLANIC REACTIONS OF SIX PRINCIPAL CLAY MINERALS: ACTIVATION, REACTIVITY ASSESSMENTS AND TECHNOLOGICAL EFFECTS," *Cem. Concr. Res. Vol. 25. No. 8, pp. 1691-1702.1*, vol. 25, no. 8, pp. 1691–1702, 1995.

[7]   D. Thesis, "Pozzolanic activity of natural clay minerals with respect to environmental geotechnics," 2005.

[8]   B. B. Sabir, S. Wild, and J. Bai, "Metakaolin and calcined clays as pozzolans for concrete : a review," vol. 23, 2001.

[9]   L. M. Vizcaíno Andrés, M. G. Antoni, A. A. Diaz, J. F. Martirena Hernández, and K. L. Scrivener, "Effect of fineness in clinker-calcined clays-limestone cements," *Adv. Cem. Res.*, vol. 27, no. 9, pp. 546–556, 2015, doi: 10.1680/adcr.14.00095.

[10]   C. S. Poon, L. Lam, S. C. Kou, Y. L. Wong, and R. Wong, "Rate of pozzolanic reaction of metakaolin in high-performance cement pastes," *Cem. Concr. Res.*,

vol. 31, no. 9, pp. 1301–1306, 2001, doi: 10.1016/S0008-8846(01)00581-6.

[11] N. Nair, K. Mohammed Haneefa, M. Santhanam, and R. Gettu, "A study on fresh properties of limestone calcined clay blended cementitious systems," *Constr. Build. Mater.*, 2020, doi: 10.1016/j.conbuildmat.2020.119326.

[12] S. Tsivilis, G. Batis, E. Chaniotakis, G. Grigoriadis, and D. Theodossis, "Properties and behavior of limestone cement concrete and mortar," *Cem. Concr. Res.*, 2000, doi: 10.1016/S0008-8846(00)00372-0.

[13] V. G. Haach, G. Vasconcelos, and P. B. Loureno, "Influence of aggregates grading and water/cement ratio in workability and hardened properties of mortars," *Constr. Build. Mater.*, vol. 25, no. 6, pp. 2980–2987, Jun. 2011, doi: 10.1016/j.conbuildmat.2010.11.011.

[14] S. Khalilpour, E. BaniAsad, and M. Dehestani, "A review on concrete fracture energy and effective parameters," *Cement and Concrete Research*. 2019, doi: 10.1016/j.cemconres.2019.03.013.

[15] K. Hanpongpun Wilasineeand Scrivener, "The Effect of Curing Temperature on the Properties of Limestone Calcined Clay Cement (LC3)," in *Calcined Clays for Sustainable Concrete*, 2020, pp. 293–298.

[16] K. Scrivener *et al.*, " Impacting factors and properties of limestone calcined clay cements (LC 3) ," *Green Mater.*, vol. 7, no. 1, pp. 3–14, 2019, doi: 10.1680/jgrma.18.00029.

[17] F. Cassagnabère, P. Diederich, M. Mouret, G. Escadeillas, and M. Lachemi, "Impact of metakaolin characteristics on the rheological properties of mortar in the fresh state," *Cem. Concr. Compos.*, vol. 37, no. 1, pp. 95–107, 2013, doi: 10.1016/j.cemconcomp.2012.12.001.

[18] M. L. Nehdi, "Clay in cement-based materials: Critical overview of state-of-the-art," *Constr. Build. Mater.*, vol. 51, pp. 372–382, 2014, doi: 10.1016/j.conbuildmat.2013.10.059.

[19] T. R. Muzenda, P. Hou, S. Kawashima, T. Sui, and X. Cheng, "The role of limestone and calcined clay on the rheological properties of LC3," *Cem. Concr. Compos.*, vol. 107, no. May 2019, p. 103516, 2020, doi: 10.1016/j.cemconcomp.2020.103516.

[20]   J. Lavanya and V. R. Rao, "Mechanical and Durability Properties of Limestone Calcined Clay Cement (Lc 3)," no. 6, pp. 359–365, 2019.

[21]   L. Qinfei, W. Han, H. Pengkun, C. Heng, W. Yang, and C. Xin, "The microstructure and mechanical properties of cementitious materials comprised of limestone, calcined clay and clinker," *Ceram. - Silikaty*, vol. 63, no. 4, pp. 356–364, 2019, doi: 10.13168/cs.2019.0031.

[22]   S. Krishnan, A. C. Emmanuel, and S. Bishnoi, "Hydration and phase assemblage of ternary cements with calcined clay and limestone," *Constr. Build. Mater.*, vol. 222, pp. 64–72, Oct. 2019, doi: 10.1016/j.conbuildmat.2019.06.123.

[23]   F. Avet and K. Scrivener, "Hydration study of limestone calcined clay cement (LC3) using various grades of calcined kaolinitic clays," in *RILEM Bookseries*, 2018, vol. 16, pp. 35–40, doi: 10.1007/978-94-024-1207-9_6.

[24]   Y. Dhandapani, T. Sakthivel, M. Santhanam, R. Gettu, and R. G. Pillai, "Mechanical properties and durability performance of concretes with Limestone Calcined Clay Cement (LC3)," *Cem. Concr. Res.*, 2018, doi: 10.1016/j.cemconres.2018.02.005.

[25]   M. Frías and J. Cabrera, "Pore size distribution and degree of hydration of metakaolin-cement pastes," *Cem. Concr. Res.*, vol. 30, no. 4, pp. 561–569, 2000, doi: 10.1016/S0008-8846(00)00203-9.

[26]   Y. Dhandapani and M. Santhanam, "Assessment of pore structure evolution in the limestone calcined clay cementitious system and its implications for performance," *Cem. Concr. Compos.*, vol. 84, pp. 36–47, Nov. 2017, doi: 10.1016/j.cemconcomp.2017.08.012.

[27]   N. Bhanumathidas, "Dual role of gypsum: Set retarder and strength accelerator Promotion of total fly ash utilisation in India View project Durability Enhancement with Complementary Cement Materials (CCMs) View project." [Online]. Available: https://www.researchgate.net/publication/287679112.

[28]   F. Cassagnabère, P. Diederich, M. Mouret, G. Escadeillas, and M. Lachemi, "Impact of metakaolin characteristics on the rheological properties of mortar in the fresh state," *Cem. Concr. Compos.*, 2013, doi:

10.1016/j.cemconcomp.2012.12.001.

[29]   G. Batis, P. Pantazopoulou, S. Tsivilis, and E. Badogiannis, "The effect of metakaolin on the corrosion behavior of cement mortars," *Cem. Concr. Compos.*, 2005, doi: 10.1016/j.cemconcomp.2004.02.041.

[30]   H. Paiva, A. Velosa, P. Cachim, and V. M. Ferreira, "Effect of metakaolin dispersion on the fresh and hardened state properties of concrete," *Cem. Concr. Res.*, 2012, doi: 10.1016/j.cemconres.2012.01.005.

[31]   S. Ng and J. Plank, "Interaction mechanisms between Na montmorillonite clay and MPEG-based polycarboxylate superplasticizers," *Cem. Concr. Res.*, 2012, doi: 10.1016/j.cemconres.2012.03.005.

[32]   B. H. Zaribaf, B. Uzal, and K. Kurtis, "Compatibility of superplasticizers with limestone-metakaolin blended cementitious system," *RILEM Bookseries*, 2015, doi: 10.1007/978-94-017-9939-3_53.

[33]   F. Nazário Santos, S. Raquel Gomes de Sousa, A. José Faria Bombard, and S. Lopes Vieira, "Rheological study of cement paste with metakaolin and/or limestone filler using Mixture Design of Experiments," *Constr. Build. Mater.*, 2017, doi: 10.1016/j.conbuildmat.2017.03.001.

[34]   B. G. Kim, S. Jiang, C. Jolicoeur, and P. C. Aïtcin, "Adsorption behavior of PNS superplasticizer and its relation to fluidity of cement paste," *Cem. Concr. Res.*, 2000, doi: 10.1016/S0008-8846(00)00256-8.

[35]   M. Collepardi, "Admixtures used to enhance placing characteristics of concrete," *Cem. Concr. Compos.*, 1998, doi: 10.1016/s0958-9465(98)00071-7.

[36]   L. Lei and J. Plank, "Synthesis and properties of a vinyl ether-based polycarboxylate superplasticizer for concrete possessing clay tolerance," *Ind. Eng. Chem. Res.*, 2014, doi: 10.1021/ie4035913.

[37]   G. Giaccio and R. Zerbino, "Optimum superplasticiser dosage for systems with different cementitious materials," *Indian Concr. J.*, 2002.

[38]   K. H. Yang, Y. B. Jung, M. S. Cho, and S. H. Tae, "Effect of supplementary cementitious materials on reduction of CO_2 emissions from concrete," *J. Clean. Prod.*, vol. 103, pp. 774–783, 2015, doi: 10.1016/j.jclepro.2014.03.018.

[39] S. Ferreiro, M. M. C. Canut, J. Lund, and D. Herfort, "Influence of fineness of raw clay and calcination temperature on the performance of calcined clay-limestone blended cements," *Appl. Clay Sci.*, vol. 169, pp. 81–90, Mar. 2019, doi: 10.1016/j.clay.2018.12.021.

[40] A. K. H. Kwan and C. F. Mora, "Effects of various, shape parameters on packing of aggregate particles," *Mag. Concr. Res.*, vol. 53, no. 2, 2001, doi: 10.1680/macr.2001.53.2.91.

[41] Q. D. Nguyen, T. Kim, and A. Castel, "Mitigation of alkali-silica reaction by limestone calcined clay cement (LC3)," *Cem. Concr. Res.*, vol. 137, no. March, p. 106176, 2020, doi: 10.1016/j.cemconres.2020.106176.

[42] P. Ptáček, F. Frajkorová, F. Šoukal, and T. Opravil, "Kinetics and mechanism of three stages of thermal transformation of kaolinite to metakaolinite," *Powder Technol.*, vol. 264, pp. 439–445, Sep. 2014, doi: 10.1016/j.powtec.2014.05.047.

[43] S. Ferreiro, D. Herfort, and J. S. Damtoft, "Effect of raw clay type, fineness, water-to-cement ratio and fly ash addition on workability and strength performance of calcined clay – Limestone Portland cements," *Cem. Concr. Res.*, 2017, doi: 10.1016/j.cemconres.2017.08.003.

[44] D. N. Huntzinger and T. D. Eatmon, "A life-cycle assessment of Portland cement manufacturing: comparing the traditional process with alternative technologies," *J. Clean. Prod.*, vol. 17, no. 7, pp. 668–675, May 2009, doi: 10.1016/j.jclepro.2008.04.007.

[45] B. S. Koelbl, M. A. van den Broek, B. J. van Ruijven, A. P. C. Faaij, and D. P. van Vuuren, "Uncertainty in the deployment of Carbon Capture and Storage (CCS): A sensitivity analysis to techno-economic parameter uncertainty," *Int. J. Greenh. Gas Control*, vol. 27, 2014, doi: 10.1016/j.ijggc.2014.04.024.

[46] N. MAHASENAN, S. SMITH, and K. HUMPHREYS, "The Cement Industry and Global Climate ChangeCurrent and Potential Future Cement Industry CO2 Emissions," in *Greenhouse Gas Control Technologies - 6th International Conference*, 2003.

[47] L. M. Vizcaíno-Andrés, S. Sánchez-Berriel, S. Damas-Carrera, A. Pérez-Hernández, K. L. Scrivener, and J. F. Martirena-Hernández, "Industrial trial to

produce a low clinker, low carbon cement," *Mater. Constr.*, vol. 65, no. 317, 2015, doi: 10.3989/mc.2015.00614.

[48]   Munfarijah Siti Isma, "Development of State of the Art-Techniques in Cement Manufacturing : Trying to Look Ahead (CSI / ECRA-Technology Papers) Final Draft 31 March 2009," *i*, no. tecnology, 2019.

[49]   E. Batuecas, F. Liendo, T. Tommasi, S. Bensaid, F. A. Deorsola, and D. Fino, "Recycling CO2from flue gas for CaCO3nanoparticles production as cement filler: A Life Cycle Assessment," *J. CO2 Util.*, vol. 45, p. 101446, Mar. 2021, doi: 10.1016/j.jcou.2021.101446.

[50]   F. Georget, W. Wilson, and K. L. Scrivener, "edxia: Microstructure characterisation from quantified SEM-EDS hypermaps," *Cem. Concr. Res.*, vol. 141, 2021, doi: 10.1016/j.cemconres.2020.106327.